Progress towards Hypoxia-Activated SN-38: The Potential to Target Hypoxic Tumors

by

Dinghua Liang

A thesis submitted to the Faculty of Graduate Studies of

The University of Manitoba

in partial fulfilment of the requirements of the degree of

Master of Science

College of Pharmacy

Rady Faculty of Health Sciences

University of Manitoba

Winnipeg

To My Mom,
who used to know me better than I did
and who foretold my beloved career during the chaos of my youth.

Abstract

Solid tumors are commonly subject to hypoxia. Hypoxic cancer cells have undesirable properties such as a high tendency to metastasize and resistance to chemotherapy and radiotherapy. Hypoxia-inducible factors (HIFs) respond to the changes in oxygen levels, orchestrating the transcription of many proteins that are vital for the survival of hypoxic cancer cells. With their parent drug SN-38 as an inhibitor of both topoisomerase 1 and HIF-1, hypoxia-activated SN-38s may have a dual inhibitory effect on hypoxic tumor cells due to hypoxia-targeting and HIF-1 inhibition.

To develop hypoxia-activated prodrugs of SN-38; 2-, 3-, and 4-nitrobenzyl SN-38s have been synthesized with good yields (78%, 67% and 68%, respectively). Topoisomerase 1 inhibitory assay on 2- and 4-nitrobenzyl SN-38s and cell viability assay on 2-, 3- and 4-nitrobenzyl SN-38s have been performed. All three derivatives showed less toxicity on K562 cells, which meets the principle of prodrug design. Cyclic voltammetry results suggest that the reduction potentials of these three derivatives may be not high enough for these compounds to be activated. The manner of reduction of three nitrobenzyl SN-38s is quasi-reversible under the testing condition, not against the proposed mechanism of activation. Two new derivatives of SN-38 have been designed to elevate reduction potential and further reduce toxicity. They are to be synthesized and tested for future work.

Acknowledgements

I wish to express my gratitude to my advisor, Dr. Geoff Tranmer, for his provision of patient training, informative instructions and financial supports.

Gratitude also gushes to my committee members, Dr. David Herbert and Dr. Emmanuel Ho. Dr. Herbert performed cyclic voltammetry experiments. Dr. Ho provided helpful comments on my work.

The methods of *in vitro* tests in this work were established by Dr. Brian Hasinoff's group. The laboratory technician Mr. Xing Wu from this group operated the majority of *in vitro* tests. Dr. Ted Lakowski and his graduate students, Ryan Lillico and Nicholas Stesco, offered numerous help with LC-MS.

Many thanks also go to Yuhua Fang, for the shared joys and thoughts; to the former laboratory technician, Jennifer Bao, for her help with my laboratory techniques and language usages; to the University of Manitoba and Government of Manitoba for kindly offering me the University of Manitoba Graduate Fellowship and Manitoba Graduate Scholarship; and, last but not least, to my parents for reasons too numerous to mention.

CONTENTS

List of Tables

List of Figures

Progress towards Hypoxia-Activated SN-38: The Potential to Target Hypoxic Tumors

Dinghua Liang

Supervisor: Dr. Geoff Tranmer

College of Pharmacy, Rady Faculty of Health Sciences

University of Manitoba

1 Introduction and Literature Review

Please be advised that part of this literature review has been revised and published as Liang, D.; Miller, G. H.; Tranmer, G. K., Hypoxia Activated Prodrugs: Factors Influencing Design and Development. *Curr. Med. Chem.* **2015,** *22* (37), 4313-4325.

1.1 Hypoxia in Tumors

Hypoxia is an oxygen-deficient state resulting in functional change of involved cells [1]. In solid tumors, hypoxia exists in certain areas of tumors due to inadequate oxygen supply caused by abnormal vasculature and irregular blood perfusion [2]. A universal standard for hypoxia has not been established because the critical oxygen concentration at which functional changes occur varies with respect to the changes of interest, with tissue O_2 partial pressure ranging from 35 mmHg (for emerging hypoxia-induced resistance to immunotherapy) to 0.02 mmHg (for

changing oxidation state of cytochromes) [1]. Although a standard for defining hypoxia has not been unanimously accepted, the metastatic aggressiveness, multi-therapeutic resistance and inferior prognosis of hypoxic tumor environments have been widely acknowledged.

Bolstered metastasis can be viewed as an adaptation of tumor cells towards the hostile hypoxic environment which lacks adequate supply of oxygen and nutrients, but accumulates metabolic wastes due to the inadequate blood flow. In fact, metastatic cancer cells are only one of the three phenotypes that result from the offspring of tumor cells facing the hypoxia-exerted clonal selection, with the other two being quiescent and apoptotic types [3, 4]. Nevertheless, the malicious metastatic phenotype is clinically the most important, and the mechanism of its ability to metastasize is worthy of consideration. Behind the unusual and undesirable behaviors of tumor cells, hypoxia-inducible factors (HIFs) respond to the changes in oxygen levels, orchestrating the transcription of many proteins that are vital for hypoxic cell's survival. Among the several prerequisites for tumor invasion, destruction of the cell-cell adhesion is one essential procedure [5] and provides a window where we can see how HIFs function. As its name suggests, hypoxia-inducible factor is activated under hypoxia, and among a myriad of its physiological functions is the extensive enhancement of expression of the lysyl oxidase that decreases the degradation of Snail (SNAI1) family proteins. The elevated level of Snail protein then suppresses the expression of E-cadherin, consequently repressing E-cadherin's function in maintaining cancer cell adhesion, and as a result, tumor invasion is facilitated [5]. Another established role of HIF is promoting angiogenesis as an attempt to ameliorate the oxygen-deficient state suffered by tumor cells. HIF encourages the expressions of two key modulators for the formation of new blood vessels, that is, angiopoietin-2 [6] and vascular epithelial growth

factor-A (VEGF-A) [7]. Angiopoietin-2 destabilizes the mature and dormant capillaries by antagonizing the vasculature-stabilizing factor angiopoietin-1, thus awakening the blood vessels from the otherwise VEGF-A-deaf state. VGEG-A then coaxes the neonatal capillaries into growing towards oxygen-deficient areas in the tumor [5]. Promoting many surviving mechanisms of hypoxic tumor cells, HIF presents itself as a desired target for anticancer therapies.

Hypoxic cancer cells not only adopt aggressive adaptations, they display resistance to many anticancer treatments as well. Systemic delivery of chemotherapy drugs can have a reduced impact on tumors, as blood-borne drugs commonly have difficulty in reaching hypoxic areas due to the abnormal vasculature and irregular blood-flowing pattern in solid tumor tissues. The therapeutic effects of radiotherapy are also compromised because of the hypoxic environment, as achieving the maximum therapeutic effects of radiotherapy requires sufficient amounts of oxygen to induce the formation of oxygen free radicals that are highly toxic to tumor cells, an effect called "oxygen enhancement effect" [1]. Without the cytotoxicity of oxygen free radicals, three times higher doses of radiation are required to produce the same therapeutic effect as is needed for normoxic cancer cells [1].

As a result of the aforementioned malignant nature and multi-therapeutic resistance of hypoxic cancers, the oxygenation state of tumors has been shown as the strongest independent prognostic factor, at least for cervical cancer [1, 8]. These facts suggest that there is an urgent necessity for a therapeutic strategy that specifically targets hypoxic tumors.

1.2 Fundamentals of Hypoxia-Activated Prodrugs

Hypoxia-activated prodrugs (HAP, also referred to as bioreductive prodrugs) are stable analogs of drugs with reduced cytotoxicity in normally oxygenated cells, but become activated and generate cytotoxins in oxygen deficient tumor cells [9]. The most extensively explored strategy for activating prodrugs under hypoxia is to utilize the chemically reducing environment in hypoxic tumor tissues [10, 11]. According to their chemical structures, bioreductive prodrugs can be categorized into four chemical classes (Figure 1-1) [9]: nitroaromatic compounds (e.g. PR-104, TH-302 and KS119), aromatic *N*-oxides (e.g. tirapazamine), aliphatic *N*-oxides (e.g. AQ4N) and quinones (e.g. apaziquone). The strategy utilizing nitroaromatic compounds is the most popular approach and will be highlighted in this review. An archetypical HAP consists of two or three functional components (Figure 1-2), namely, a trigger, linker (optional) and effector [12]. In the case of nitroaromatic HAPs, the trigger is a nitroaromatic group, the effector is a warhead to be activated or drug to be discharged, and the linker connects the two, and is sometimes omitted. The activating mechanism of nitroaromatics involves the phenomenon that the electron density on the aromatic moiety increases dramatically when a strongly electron-withdrawing nitro group is reduced to a weakly electron-donating group, such as a hydroxylamine, by certain reductases (*vide infra*). It is this elevation of electron density that results in the activation or detachment of the effector. In this activating process, the inversion of the electron-withdrawing to electron-donating effects is aptly termed "electronic switch" [13, 14].

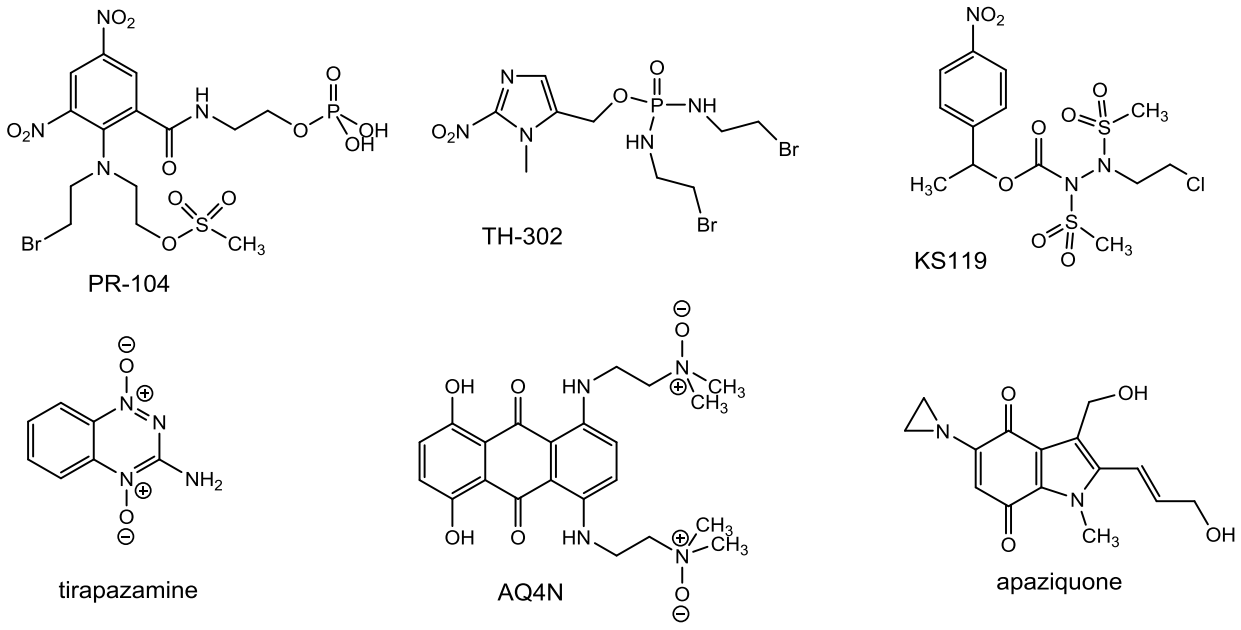

Figure 1-1 Structures of HAP examples

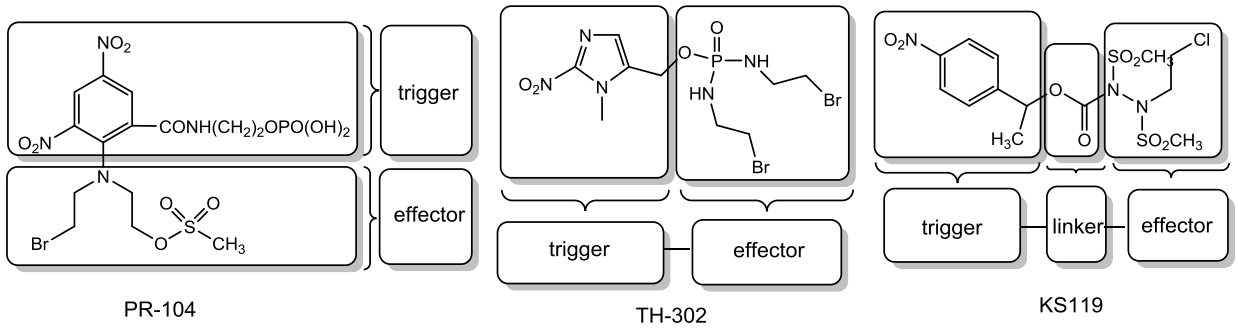

Figure 1-2 Functional components shown in three nitroaromatic HAP examples

Describing the mechanism of HAP's selectivity towards hypoxic cells, however, requires more details of the activating process. In hypoxic environments, certain reductases, such as NADPH:cytochrome P450 oxidoreductase, reduce a nitro HAP in a one-electron manner to produce a radical anion (Figure 1-3). With the help of protons, the radical anion can be converted to a nitroso compound [14, 15] and then undergoes further reductions to form a hydroxylamine or amine [9, 14]. In normoxic tumor cells, however, the drug reduced by these

enzymes are readily oxidized back to its parent prodrug by oxygen [16], thus forming a process called "futile redox cycle" [9]. Of note, during this futile redox cycle, oxygen molecules are reduced to superoxide, which is a free radical that damages cells [17] and can cause background toxicity. Fortunately, superoxide can be detoxified by the ubiquitous enzyme superoxide dismutase [18].

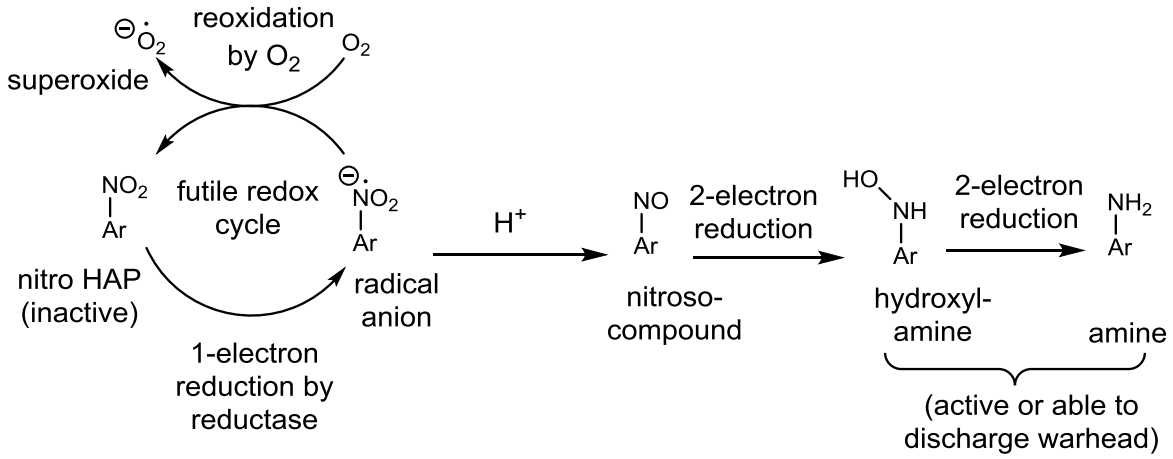

Figure 1-3 Simplified process of activation
Ar, substituted aromatic ring

1.3 Factors Influencing Design and Development of HAP

Many efforts have been made to pin down the key parameters for developing a successful HAP. These efforts have revealed that one-electron reduction potential (E^1) affects the selectivity between hypoxic and normoxic cells and hence the cytotoxicity; both the prodrug and active drug's stability and diffusibility play important roles in governing a HAP's efficacy. A rational design for an effective HAP should include these properties into considerations.

1.3.1 One-Electron Reduction Potential

An appropriate one-electron reduction potential (E^1) is vital for a HAP to be not only efficiently activated by reductases and exert therapeutic effects in hypoxic cells but also readily reoxidized by oxygen to prevent undesirable toxicity in normal cells. Reduction potentials cited in this section are all values vs. normal hydrogen electrode (NHE), unless indicated otherwise. The first step of reduction in which nitroaromatics are reduced to nitroso compounds is believed to be the rate-limiting step [15]. The following reductions in which nitroso aromatic compounds are reduced to hydroxylamines is considered as a facile process because reduction potentials of nitroso aromatics are markedly higher than that of their nitro counterparts [15]. For example, reduction potentials of nitrobenzenes fall within the range of -0.58 ~ -0.81 V, whereas the range of nitrosobenzenes is +0.04 ~ +0.25 V [19]. Therefore, the nitroaromatics' one-electron reduction potentials determine the rate of the first reduction step, and determine the entire activating process as well. Too low a reduction potential of a HAP, especially when significantly lower than that of reductases (E^1 = -220 ~ -310 mV, see below for details), hinders the activation; however, too high a reduction potential makes the reducing process too fast and thus out of the harness by oxygen (the effective E^1 (O_2) is -155 mV, a value of a nonstandard state of 1 mole/dm^3; the standard state of O_2 is 1 atmosphere, which is inappropriate for comparison with drugs in solutions [20]). A multiple linear regression analysis of 35 nitroaromatics indicates that an increase of 100 mV in reduction potentials enhances the potency approximately by 10 folds, but the aerobic toxicity also increases correspondingly [21]. Therefore, an empirical range of reduction potentials for HAPs is usually suggested as -400 to -200 mV [14, 15] or as a lower and narrower window between -450 and -300 mV [16, 22]. Some tissues such as bone marrow [23-25], esophagus [26], retina [27] and skin [28] are mildly hypoxic under normal physiological conditions

and therefore susceptible to HAPs. To circumvent the potential toxicity to these physiologically hypoxic tissues, the therapeutic strategy targeting severe hypoxia can be adopted by modifying reduction potentials of HAPs to fall within the lower window.

The one-electron reduction potential of mono-nitro-substituted phenyl compounds could be too low (e.g. nitrobenzene, E^1 = -486 mV [29]) to be used as the trigger. To elevate the reduction potentials of nitroaromatic compounds, two methods are usually used. The most straightforward method is to introduce additional electron-withdrawing substituents into the mono-nitro-benzene trigger, which is the strategy adopted in designing the PR-104 that carries three electron-withdrawing moieties: two nitro and an aminocarbonyl groups. Although there is no available value of PR-104's reduction potential, the datum of a structurally similar compound 3,5-dinitrobenzoic acid (E^1 = -344 mV [29]) can be considered for rough reference. Another strategy is substituting nitrobenzene with nitroheterocycles that have intrinsically higher reduction potentials (e.g. 2-methyl-5-nitrofuran, E^1 = -330 mV and 1-methyl-2-nitro-1H-imidazole, E^1 = -389 mV; [21]). TH-302 is an excellent example of nitroheterocyclic HAPs with an appropriate one-electron reduction potential E^1 = -407 mV [30].

1.3.2 Diffusibility and Stability of the Prodrug

The characteristic abnormal vascularization in hypoxic regions raises the problem of transporting HAPs to hypoxic cells. Amounts of HAP delivered to hypoxic regions depend on two major factors: the diffusibility and stability of prodrug [9].

Once a prodrug is carried by the blood flow to the end of vasculature, passive diffusion becomes the major form of drug transportation. Therefore, the prodrug molecule's ability to diffuse plays

a crucial role in shaping the front line of the battle against hypoxic tumors. The HAP's diffusibility depends on its diffusion coefficient that is primarily a function of the compound's lipophilicity (log *P*, octanol/water partition coefficient) and is secondarily influenced by the number of hydrogen bond donors and accepters in the structure, molecular weight of the prodrug, and density of the cell layer through which the prodrug diffuses [31]. For the aromatic *N*-oxide HAP, tirapazamine, the function between diffusion coefficient and log *P* can be mapped as a sigmoidal curve, in which the diffusion coefficient surges with the increase of lipophilicity between log *P* values -2 ~ 2 but changes very little out of this range. At a given log *P* value, addition of both hydrogen bond donors and acceptors into the structure impairs the diffusibility, with the installation of hydrogen bond donors producing more profound decreasing effects. Larger molecules have weaker ability to diffuse; however, the influence of molecular weight is insignificant, at least in the range between 200 to 500 daltons. Diffusions in cell lines with higher packing density are more readily subject to the impact of lipophilicity, perhaps because in these cell lines, drugs diffuse almost exclusively through lipophilic membranes, whereas in loosely packed cell layers both lipo- and hydrophilic molecules can permeate alternatively via the route of paracellular flux.

An appropriate level of stability is also a necessary property for a successful HAP. If the prodrug's structure is too robust, it may remain inactive even in hypoxic conditions. However, a too readily metabolized HAP may dissipate considerably along its march to the target cells or even be activated prematurely.

1.3.3 Stability and Diffusibility of the Active Drug

Even after a prodrug has been activated, stability and diffusibility of the active drug still influence its efficacy, by determining the extent of a phenomenon called "bystander effect". In the setting of targeting hypoxia, the term "bystander effect" refers to "the killing of adjacent cells that lack prodrug-activating ability through local diffusion of the active drug" [9]. When exploited effectively in designing severe-hypoxia-targeting HAPs, bystander effect can expand these HAPs' antitumor effects beyond just severely hypoxic tumor cells and include moderately or mildly hypoxic tumor cells as well. In fact, it is estimated that nearly half (30% in SiHa cervical cancer cells and 50% in HCT116 colon cancer cells) of the therapeutic activity of PR-104 is credited to bystander effects[32].

Stability of the active drug is the prerequisite for bystander effects to exist, as active drugs must survive the diffusion journey before they can wield their warheads towards normoxic cells. Stable drugs are more likely to reach less hypoxic regions than are the highly reactive ones. For example, the relatively stable bromo-isophosphoramide mustard (Br-IPM) (Figure 1-5) as the active drug of TH-302 allows this HAP to possess an intermediate level of bystander effect [30]. By contrast, the active metabolites of the aromatic *N*-oxide HAP, tirapazamine, which are believed to be highly reactive free radical species such as hydroxyl radical [33] and benzotriazinyl radical [34], lead to nearly no bystander effects being found [35]. Structural features affecting the diffusibility of active drugs are expected to be similar to those of prodrugs.

1.4 Select Examples of Nitroaromatic HAPs

The electronic switch effect on nitroaromatic moieties changes HAPs' physiochemical property and physiological activity by two mechanisms: either by modifying the structure directly on the parent compound or by separating the prodrug molecule into several parts containing the active drug. The latter fragmenting mechanism is more attractive at least in principle, because the more dramatic change in structures is expected to be associated with more distinguishable differences in cytotoxicity or pharmacokinetic properties from those of the prodrug. Among the following examples of nitroaromatic HAPs, PR-104 is activated by the direct-modifying mechanism, whereas TH-302 and KS-119/KS-119W fragment to discharge active warheads in hypoxic cells.

1.4.1 PR-104

PR-104 is a water-soluble phosphate ester of a non-symmetric dinitrobenzamide mustard, characteristically carrying a bromide and mesylate substituents as active leaving groups (Figure 1-4). PR-104 exerts cytotoxicity as a DNA cross-linking agent and has ca. 10- to 100-fold potency differentials towards different cancer cell lines [36]. PR-104 functions as a preprodrug on which its solubility-enhancing phosphate moiety is rapidly hydrolyzed ($t_{1/2}$ ca. 3 min after i.v. in mice [36]) to the prodrug PR-104A which is a less water-soluble alcohol. PR-104A is then activated in hypoxic cells by a group of possible reductases including POR [37], MTRR [38], iNOS [38], NDOR1 [38] and FOXRED2 [39] (*vide infra*). Of note, the activation of PR-104A by another reductase AKR1C3 (aldo-keto reductase 1C3) [40] is hypoxia-independent because of the nature of 2-electron reduction, which presumably enfeebles the hypoxic selectivity [40]. The major reduced and active metabolite is the *para*-hydroxylamine PR-104H, which in turn undergoes a series of nucleophilic substitutions and generates a family of metabolites, among which the halogenated compounds **1**, **2** and further reduced amine **3** (Figure 1-4) are even more potent than

their parent molecule PR-104H [36]. Moreover, compounds **1**, **2** and **3** are more lipophilic and concentrated in extracellular distribution than is PR-104H and therefore are believed to be the major contributors for the bystander effects that accounts for about half of PR-104's cytotoxic effects [32]. Although PR-104 is a promising nitroaromatic HAP, currently its progress is halted in four phase 2 clinical trials due in large part to poor tolerance. (www.clinicaltrials.gov identifiers: NCT00862082, NCT00544674, NCT00862134 and NCT01037556)

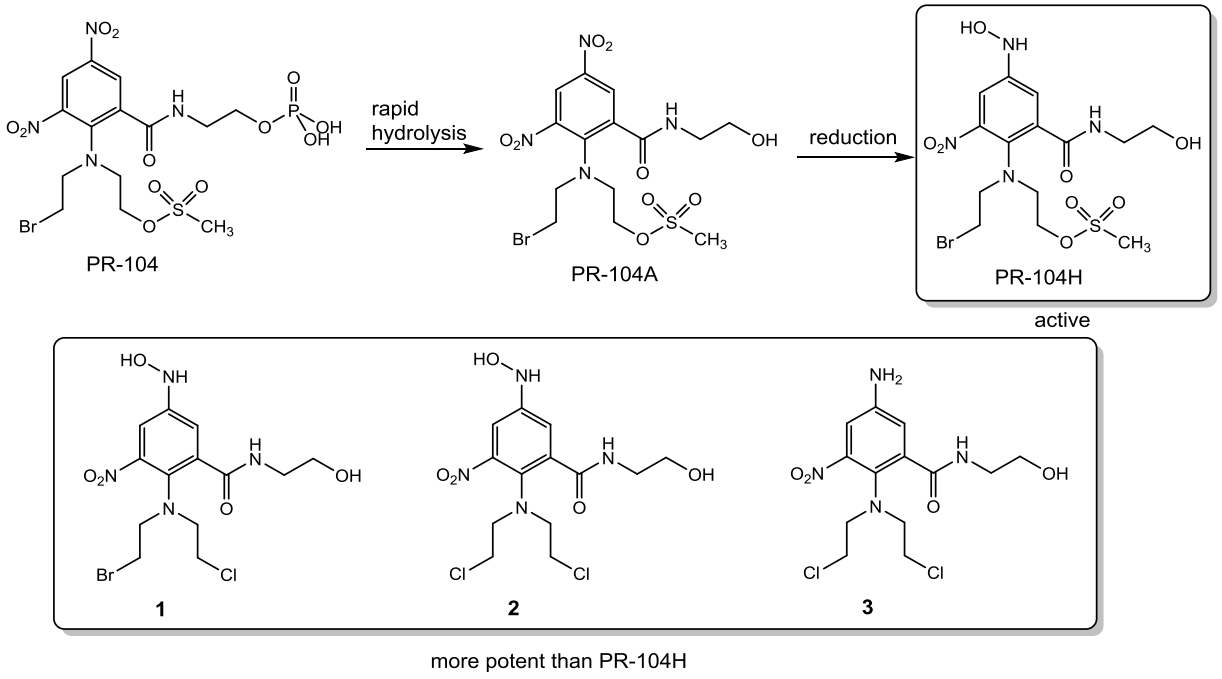

Figure 1-4 Structures of PR-104 and important metabolites

1.4.2 TH-302

TH-302 (evofosfamide) is a nitroimidazole-triggered phosphoramidate mustard, with two bromoethyl-monosubstituted nitrogen atoms joined with a phosphoryl group (Figure 1-5). It is currently the most advanced nitroaromatic HAP in terms of progress in clinical trials. It has completed two phase 3 clinical trials in combination with gemcitabine for treating pancreatic adenocarcinoma and with doxorubicin for soft tissue sarcoma (www.clinicaltrials.gov identifier:

NCT01746979 and NCT01440088, respectively). Unfortunately, TH-302 did not meet primary overall survival endpoints in these two phase 3 clinical trials [41].

Carrying a 2-nitroimidazole as the trigger and liberating a phosphoramide as the warhead, TH-302 is a HAP exploiting a nitroheterocycle-triggering and fragment-killing strategy. One-electron reduction caused by radiolysis leads to the detection of the warhead bromo-isophosphoramide mustard (Br-IPM), "trigger-H" and "trigger-dimer" as the fragments (Figure 1-5), suggesting that the activating mechanism probably involves the formation of a "benzyl-type radical" derived from a radical anion that is the initial one-electron-reduced intermediate [30]. Metabolism study on rats confirmed that Br-IPM was among the metabolites [42]. Further studies revealed the DNA cross-linking effect as the major cytotoxic mechanism of Br-IPM [30], in agreement with the previous expectation derived from TH-302's bifunctionalized structure [43]. The bystander effect is also believed to participate in the therapeutic action, supported by the findings from tests in multicellular layer [30] and mice [44]. TH-302 has an excellent hypoxic selectivity with hypoxia cytotoxicity ratio (HCR) of more than 200 towards certain tested cancer cells such as H460 and HT29 cells [43]. This favorable hypoxic selectivity probably originates from TH-302's relatively low one-electron reduction potential (E^1 = -407 mV [30]), which stringently confines its activating region to severe hypoxic cell clusters. Although POR is believed to be the main activating enzyme [30, 45], evidence also suggests FOXRED2 [39] and MTRR [38] may be involved in this HAP's activation.

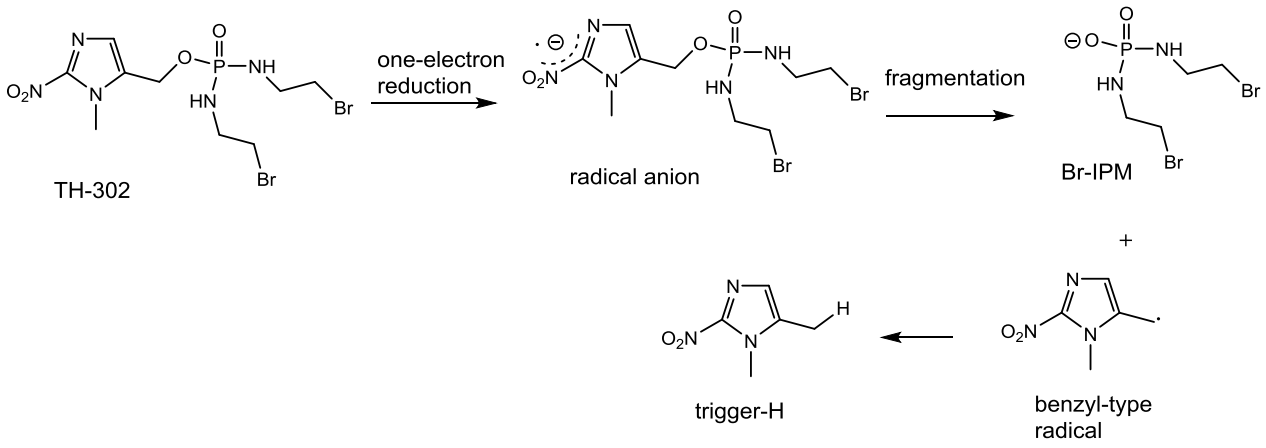

Figure 1-5 The process of activation of TH-302

Finally, it is worthy of reviewing the structure-activity relationship of compounds around TH-302. Interestingly, both higher potency and selectivity are biased toward the 2-nitroimidazole triggered TH-302 than its 5-nitroimidazole triggered isomer [43], presumably because 5-nitroimidazole is difficult to be activated as a result of its unfavorably lower one-electron reduction potential (*cf.* -483 mV for *N*-methyl-5-nitroimidazole methanol and -421 mV for *N*-methyl-2-nitroimidazole methanol [46]). With two bromine atoms as better leaving groups, TH-302 is 10-fold more potent than its dichloro-substituted cousin [43]. Monosubstitution on each nitrogen atom is essential for stability, because further alkylated compounds are susceptible to oxidation by microsomal cytochrome P450 enzymes, probably due to enhanced microsomal uptake facilitated by improved lipophilicity of the further alkylated compounds [43].

1.4.3 KS119/KS119W

KS119 is a nitrobenzyloxycarbonyl derivative of a hydrazine alkylator 90CE (Figure 1-6), whereas KS119W is a water-solubility-enhanced version of KS119, with a hydrophilic phosphate group installed on the benzene ring [47]. All the three functional components of HAP are

conspicuously shown on KS119/KS119W (Figure 1-6): a nitrobenzyl trigger, a carbamate linker and an alkylating warhead [48]. With POR, NADH:cytochrome *b*5 reductase and xanthine oxidase as possible activating enzymes [49], KS119 is postulated to be reduced to a hydroxylamine, subsequently decomposing to three parts: hydroxyl imine, carbon dioxide and the substituted hydrazine 90CE (Figure 1-7) [49]. The unstable 90CE then rapidly undergoes elimination to generate a series of reactive ethylating species that cause guanosine-cytosine cross-links [50]. As a result of this rapid metabolism, 90CE is short-lived ($t_{1/2}$ = ca. 30 seconds, at pH 7.4 and 37 ℃[48]) and therefore unlikely to exhibit bystander effect, which might be a drawback in consideration of its activation under severe hypoxia resulted from the relatively low reduction potential (half-wave reduction potential $E_{1/2}$ = -415 and -575 mV, measured on a racemic mixture [48]). However, KS119 differentiates itself from the other DNA cross-linking agents because it shows strong toxicity to cancer cells with alkylator resistance mediated by O^6-alkylguanine-DNA alkyltransferase, despite the fact that only 40% of KS119 is activated in cancer cells under experiment-induced hypoxia [51].

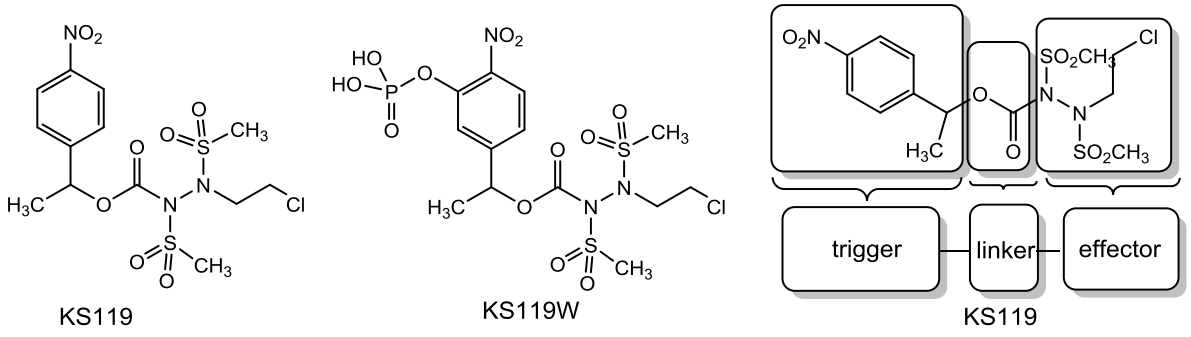

Figure 1-6 Structures of KS119 and KS119W

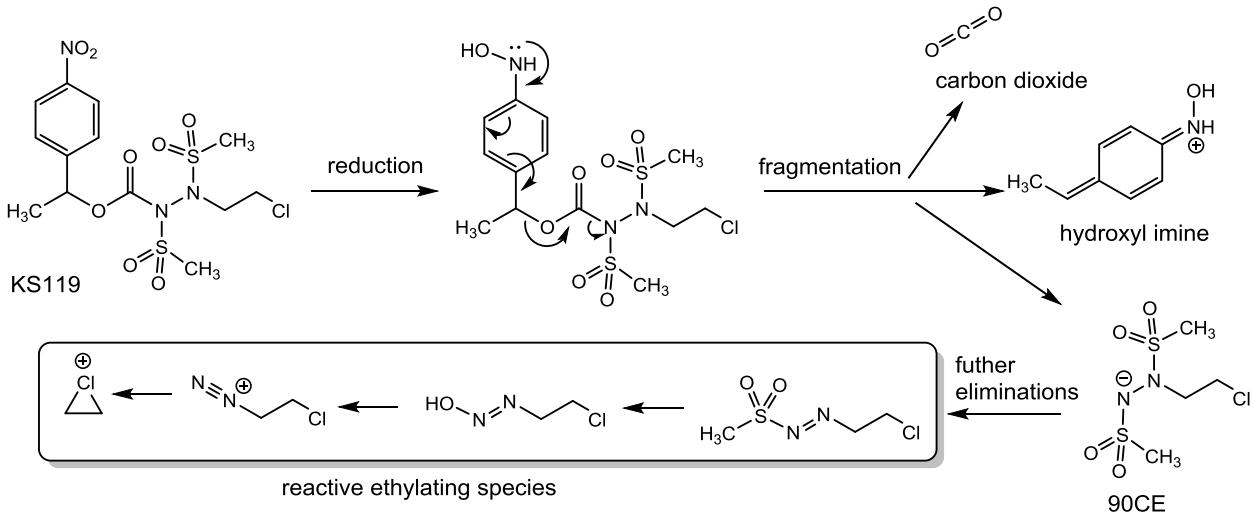

Figure 1-7 The process of activation of KS119

Another example of KS119's uniqueness among HAPs is that it has a pair of atropisomers that act as separate chemical species , as they have different conformations that cannot convert into each other on the timescale of cellular exposure because of hindered bond rotation [48]. This hindered bond rotation is believed to originate from the expulsion between the carbonyl group and methyl moiety at the benzyl carbon atom (Figure 1-8), wherein the methyl group is installed to obstruct the undesired activation by thiolysis of glutathione via an S_N2 process catalyzed by glutathione *S*-transferase [52]. These two atropisomers show 14% difference in their values of partition coefficient, which are different enough for them to be separated via HPLC equipped with a C18 reverse-phase column. Most importantly, when exposed to an equilibrium mixture of the atropisomers, the examined EMT6 cell line responds diversely to the cytotoxic effects of individual atropisomer, with 7-fold stronger sensitivity to the more lipophilic conformation that is supposed to be more readily to be taken up and metabolized. The atropisomers' corresponding conformations have been postulated as an "open form" with larger lipophilicity and stronger cytotoxicity and a "closed form" with the opposite properties (Figure 1-8).

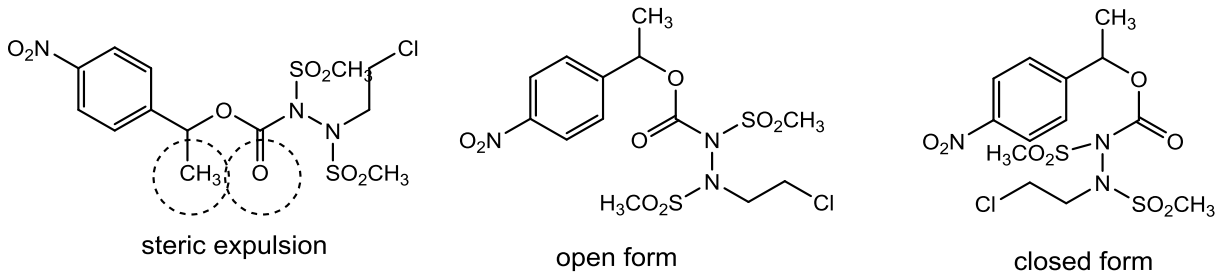

Figure 1-8 Structures of KS119 showing the steric expulsion between the methyl and carbonyl groups, and the pair of atropisomers

1.5 HAP-Activating Enzymes

Free radicals (compounds with unpaired electron(s)) are usually very unstable and therefore highly reactive. This high reactivity is the pushing force for one-electron-reduced HAP to be readily reoxidized by oxygen in normoxic cells, resulting in the origin of HAPs' hypoxic selectivity. Paradoxically, this highly unstable stage in the HAP-activating process also means the pivotal radical intermediates are difficult to form. In principle, more readily achieved two-electron reductions can compete with, and may even win out over, the desired one-electron reductions. This is evidenced by the compromised hypoxic selectivity of PR-104 because of the competitive two-electron reduction catalyzed by the enzyme AKR1C3 [40]. Knowledge of HAP activating enzymes is therefore crucial to HAP design. For example, understanding of the enzymes' electron-acceptor-binding domain will form a firm foundation for improving the prodrugs' affinity to one-electron reductases, allowing for the possibility of highly hypoxia-selective HAPs. In spite of this very promising vista, however, currently very few questions about these enzymes have been answered satisfactorily, although at least four one-electron reductases (POR [45], MTRR [38], NDOR [53] and iNOS [54], see individual descriptions below for details) have exhibited possible involvement in the HAP-activating process. Whereas POR is anchored on endoplasmic reticulum membrane, the other enzymes can all be found in cytoplasm,

indicating that these four reductases are readily accessible to bioreductive drugs. With the ability to reduce nearly all studied bioreductive prodrugs [9], POR had normally been regarded as the major HAP reductase. However, its importance was recently challenged by the interrogation of a new research method using POR-knockout strategy [45].

All the four relevant one-electron reductases belong to a family of enzymes called diflavin reductases that characteristically utilize two flavin cofactors, a flavin adenine dinucleotide (FAD) and flavin mononucleotide (FMN), in tandem to transfer the electronic flux flowing from NAD(P)H to the electron acceptors [55] that are bioreductive prodrugs in our context. The principle of the reduction mechanism of these four reductases is the same and can be depicted in a general view. Within the active site of these enzymes, a pair of electrons donated by NAD(P)H in form of hydride is accepted by the FAD where one electron of the pair is then held in the FAD's isoalloxazine ring, and the other electron jumps to the adjacent FMN where this electron is finally transferred to bioreductive drugs [55]. The cooperation between the two flavin cofactors is essential for carrying out the reduction in a one-electron manner. Although these diflavin reductases share a same catalyzing mechanism, their other properties diverge in terms of reduction potentials of the catalytic sites and catalyzing efficiency. As a result of the FMN group being the site directly delivering an electron to bioreductive prodrugs, the reduction potentials of the FMN group in these reductases are the most pertinent parameters for the activation of bioreductive prodrugs. Reduction potentials of FMN group [semiquinone/ hydroquinone] of NDOR1 [56], POR [57], iNOS [58] and MTRR [59] are -305, -269, -245 and -227 mV, respectively. At first sight, these reduction potentials may appear to be too high for these enzymes to reduce HAPs, as reduction potentials for HAP design are suggested as the ranges of

-400 ~ -200 mV [14, 15] or -450 ~ -300 mV [16, 22]. However, it has been postulated that for reductions that have been designed to take place within tumor cells, many other factors intervene to offset this impotence, such as abundant NAD(P)H or a driving force (e.g. product diffusion). In fact, despite possessing the lowest FMN reduction potential among the four enzymes, NDOR1 is not the most effective one-electron reductase. POR is the most active catalyst in this group, with ca. 100-fold higher catalyzing efficiency than the three remainders [53, 60, 61]. Other information about these enzymes, such as physiological functions and metabolizing importance to HAPs, will be reviewed individually for POR, MTRR, NDOR1 and iNOS. Two other HAP-reduction-relevant enzymes, FOXRED2 and AKR1C3, will also be discussed.

1.5.1 NADPH:Cytochrome P450 Oxidoreductase (POR)

NADPH:cytochrome P450 oxidoreductase (POR, also CPR or CYPOR), which is the first discovered diflavin reductase, is able to deliver an electron from NADPH to a variety of acceptors [55]. As a cofactor for a variety of other enzymes, POR donates an electron to cytochrome P450 enzymes (hence its name) that metabolize drugs, to cytochrome b_5 that supports the function of fatty acid desaturase and elongase, to heme oxygenase that degrades hemes, to squalene monooxygenase that synthesizes sterols, and directly to several HAPs that are activated in this electron-transferring process [62]. POR is the best-studied reductase among HAP-activation-related enzymes. With the highest catalytic activity among the four diflavin reductases, POR was supposed to be the major activating enzyme for many HAPs, and overexpression of POR in different cell lines indeed shown to be corresponding to enhanced activations of many structurally diverse HAPs including benzotriazine *N*-oxides (e.g. TPZ [63]) and nitroaromatics (e.g. PR-104A [37], TH-302 [30] and KS119 [49]). Nearly half of PR-104A's reduction was estimated to be catalyzed by POR [37]. However, further attempts to quantify

POR's contribution to HAP reduction cast doubts on its importance. In a recent study, only two of nine examined POR-reducible HAPs exhibited that their activations were strongly dependent on POR's activity; other HAPs, including PR-104A and TH-302, showed only modest differences in levels of activation between POR-knockout and -intact cells [45]. In addition, POR's role in HAP activation is complicated further if the divergent levels of POR expression among different cancer cells are taken into consideration. Surgical tumor samples usually show low levels of POR expression, with exceptions that relatively high levels of POR expression are found in ovarian and liver cancer cells [38]. Furthermore, it is difficult to extrapolate the metabolism pattern to structurally related compounds, as indicated by the distinct responses of structurally similar dinitrobenzamides, CB1954 and PR-104A, to POR knockout (Figure 1-9), in which reductive metabolism dropped markedly for CB1954 but altered only slightly for PR-104A [45].

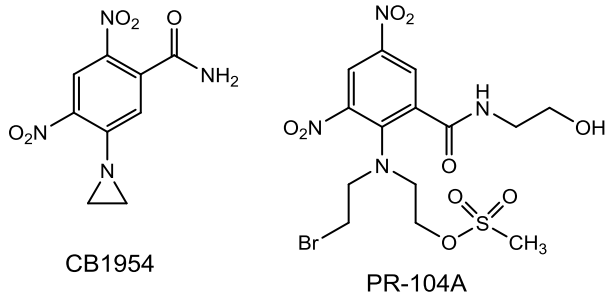

Figure 1-9 Structures of CB1954 and PR-104A

1.5.2 Methionine Synthase Reductase (MTRR)

Methionine synthase reductase (MTRR, also MSR) is in charge of reductive activation of mammalian methionine synthase that methylates homocysteine to methionine with the supernucleophilic cob(I)alamin as a transporter for methyl group [61]. The electron-rich nature of cob(I)alamin makes methionine synthase subject to oxidation and necessitates the reductive

activation by MTRR. In addition to possessing this major physiological function, MTRR is also able to activate certain HAPs such as PH-104A [38] and perhaps TH-302 [38] and therefore a possible contributor to HAP activation. However, this possibility is enfeebled by MTRR's poor expression in a panel of 23 examined cancer cells, although expression of its corresponding mRNA can be detected in a wide spectrum of human tumor cells [38].

1.5.3 NADPH Dependent Diflavin Oxidoreductase 1 (NDOR1)

NADPH dependent diflavin oxidoreductase 1 (NDOR1) was initially named novel reductase 1 (NR1) by its discoverers [64]. The physiological function of NDOR1 is unclear, except for some evidences implying that its function may overlap with that of MTRR in activating methionine synthase [65]. Interestingly, its discoverers predicted that NDOR1 would possibly be an activating enzyme for bioreductive prodrugs because it expressed widely in human cancer cells [53]. Indeed, NDOR1 has been demonstrated to be able to activate PR-104A. Similar to the case of MTRR in the same study, however, evidence of NDOR1's expression in the 23 tested cells is faint, and only under unusually intensified experimental condition can any sign of its expression be seen [38].

1.5.4 Inducible Nitric Oxide Synthase (iNOS)

Nitric oxide synthases (NOS) are three isoforms of enzymes that catalyze the formation of nitric oxide. The three isozymes are inducible NOS (iNOS, also NOS2A), endothelial NOS (eNOS) and neuronal NOS (nNOS) founded in macrophage, endothelium and neurons, respectively [66]. What makes iNOS distinct from the other two members is that some properties support iNOS to be a stable contributor to HAP activation because it maintains high activity once it is generated, whereas the activities of eNOS and nNOS are subject to the regulation of calcium or calmodulin [58]. In addition, high levels of iNOS expression have been found in breast [67] and bladder [68]

cancer cells. PR-104A [38], CB1954 [69] and tirapazamine [70] have been suggested as possible substrates of iNOS, although in the case of PR-104A, no signs of iNOS native expression were detected in the 23 cancer cell lines in which activations of PR-104A were tested [38].

1.5.5 FAD-Dependent Oxidoreductase Domain Containing 2 (FOXRED2)

FAD-dependent oxidoreductase domain containing 2 (FOXRED2) is a recently discovered flavoprotein, also known as endoplasmic reticulum flavoprotein associated with degradation (ERFAD) [71]. Located in the endoplasmic reticulum lumen, FOXRED2 is supposed to be involved in facilitating the degradation of ill-synthesized proteins. Unfolding these unqualified proteins is believed to be a necessary pretreatment for performing further degradations. Opening the protein bends necessitates the help of a reductase to reduce the disulfide bonds between the folded peptide chains, allowing the reductase FOXRED2 to perform its role [71, 72]. Whereas FOXRED2 is not a diflavin reductase, evidence supports that it can activate HAPs, including PR-104A and TH-302, by one-electron reduction [39]. Of note, TH-302's cytotoxicity increases more significantly in normoxic than hypoxic conditions. This suggests that FOXRED2 might contribute very little, if any, to TH-302's hypoxic selectivity [39]. Although high levels of expression were found in cancer cells in lung, colon, breast and pancreas [39], the fact that FOXRED2 is buried deeply in the endoplasmic reticulum lumen presumably implies that only HAPs with apparent bystander effect, such as PR-104A and TH-302, can benefit from FOXRED2's activation [39], and generate a strong bystander effect, as these drugs can readily diffuse out of the endoplasmic reticulum and reach their targets of action after being activated.

1.5.6 Aldo-Keto Reductase 1C3 (AKR1C3)

Competitive two-electron reduction of HAP is one major unwanted shunt of HAP activation, as this reduction process is refractory to reoxidation in normoxic cells, which is the origin of

hypoxic selectivity. Aldo-keto reductase 1C3 (AKR1C3) is an example of two-electron reductases that may compromise hypoxic selectivity. AKR1C3 is a member of a superfamily of NAD(P)H-linked oxidoreductases called aldo-keto reductases (AKRs) that reduce ketones or aldehydes to alcohols [73]. Specifically, AKR1C3 is in charge of reducing 17-ketosteroid to 17β-hydroxysteroid and synthesizing prostaglandin F [73]. No nitroaromatic compounds have been confirmed as its substrates until the emergence of evidences showing that AKR1C3 activates the dinitrobenzamide HAP, PR-104 [40]. Interestingly, no other nitroaromatic HAPs, including TH-302, have been proved to be substrates of this reductase. In normal tissues, high levels of expression of AKR1C3 have been found in the intestine and kidney; other important tissues that express AKR1C3 are liver and bone marrow [40]. Perhaps this relatively wide distribution in vital organs is the cause of the poor tolerance of PR-104, which led to the termination of this prodrug's clinical trials in phase 2 stage (see above). However, this drawback may be accompanied by opportunities as well. AKR1C3-related PR-104 sensitivity under aerobic conditions has been found in five cancer cell lines (A549, H460, SiHa, 22Rv1, and HT29) [40], suggesting that PR-104 may still have chemotherapeutic benefit if administrated locally to these tumors.

1.6 Camptothecins: Mechanisms of Action

Camptothecins (Figure 1-10) are a family of compounds structurally related to the natural alkaloid camptothecin. Camptothecin was initially extracted from the tree *Camptotheca acuminata* native to Southern China, but its promise of clinical application was precluded by its poor water-solubility. Many efforts therefore have exerted to overcome this limitation and eventually resulted two clinically approved and widely prescribed camptothecin derivatives,

topotecan (Hycamtin) and irinotecan (Camptosar) [74]. Topotecan has been approved for treating ovarian cancer and small-cell lung cancer, whereas irinotecan is a second-line agent for advanced colorectal cancer refractory to fluorouracil [74]. In terms of pharmacological mechanism, camptothecins are inhibitors of topoisomerase 1 [75], but evidence also suggests that they can inhibit the expression of hypoxia-inducible factor 1 [76, 77]. The following sections will provide a brief description of camptothecins' anticancer mechanism and discuss the strategy for developing hypoxia-activated camptothecin prodrugs.

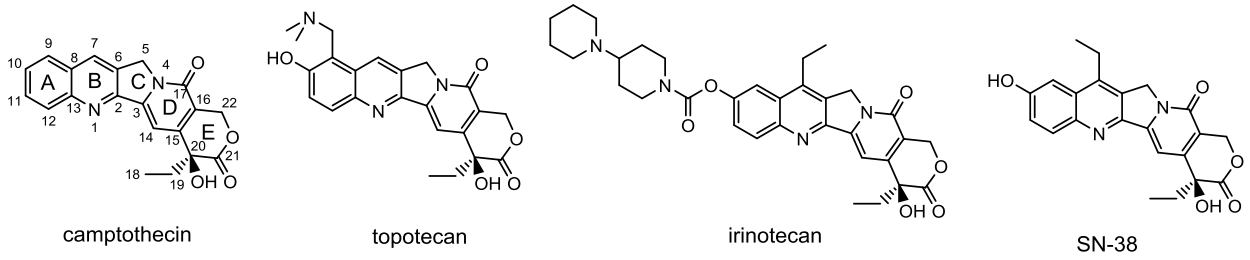

Figure 1-10 Structures of relevant camptothecins

1.6.1 Inhibition of Topoisomerase 1

During DNA replication, a twisted DNA double stand becomes unwound and opens to separate strands, in order to allow a single strand to serve as a template for DNA synthesis. However, a torsional stress can build up ahead of the replication fork as a result of the movement of the DNA polymerase along the DNA double strand (Figure 1-11) [74]. Accumulation of this torsional stress will eventually discontinue the DNA synthesis. Topoisomerase 1 resolves this problem by cutting a nick on one DNA strand; and the torsional stress can then be released by an ATP-independent rotation of the broken DNA around the remaining unbroken strand. The formation of the single-strand nick is the consequence of the nucleophilic attack by a phenyl hydroxyl group of tyrosine residue (Y723) of human topoisomerase 1 on a phosphoryl group that links two

deoxynucleotides, resulting a phosphotyrosine covalent enzyme-DNA complex with a free 5'-hyroxyl group at the 3' side of the DNA break (Figure 1-12) [75, 78]. In spite of the covalently bonded nature, this complex is readily destroyed and the intact DNA double strand restores because of the much more favored reattack from the neighboring 5'-hydroxyl group. This binary enzyme-DNA complex can be stabilized by camptothecins. Camptothecins can form hydrogen bonds with the topoisomerase 1 and π-π stacking interactions with the base pairs in the DNA double strand [75]. As a result of the binding, the distance between the two base pairs beside the single-strand nick increases from 3.6 Å to 7.2 Å to accommodate the intercalated camptothecin [75]; moreover, the twist angle between these two base pairs decreases from 39° to 10° (tending to be parallel) to achieve maximal overlap with the drug [78]. The combined effect of increase in distance and decrease in twist angle elongates the distance between the 5'-hydroxyl group and the 3'-phosphotyrosine from 3.5 Å to 11.5 Å (Figure 1-13), significantly lowering the possibility of the reattack by 5'-hydroxyl group [75]. This enzyme-drug-DNA ternary complex eventually collides with the replication fork, causing a double-strand cleavage which is lethal to cancer cells [74, 79].

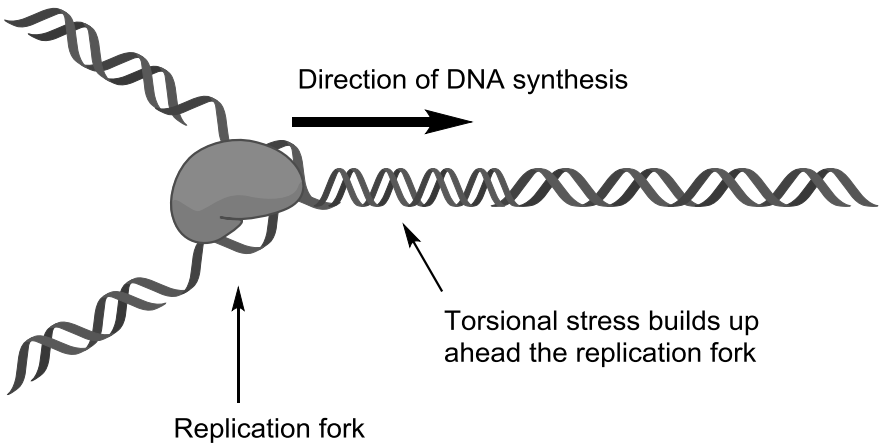

Figure 1-11 A schematic diagram showing the accumulation of torsional stress during DNA replication

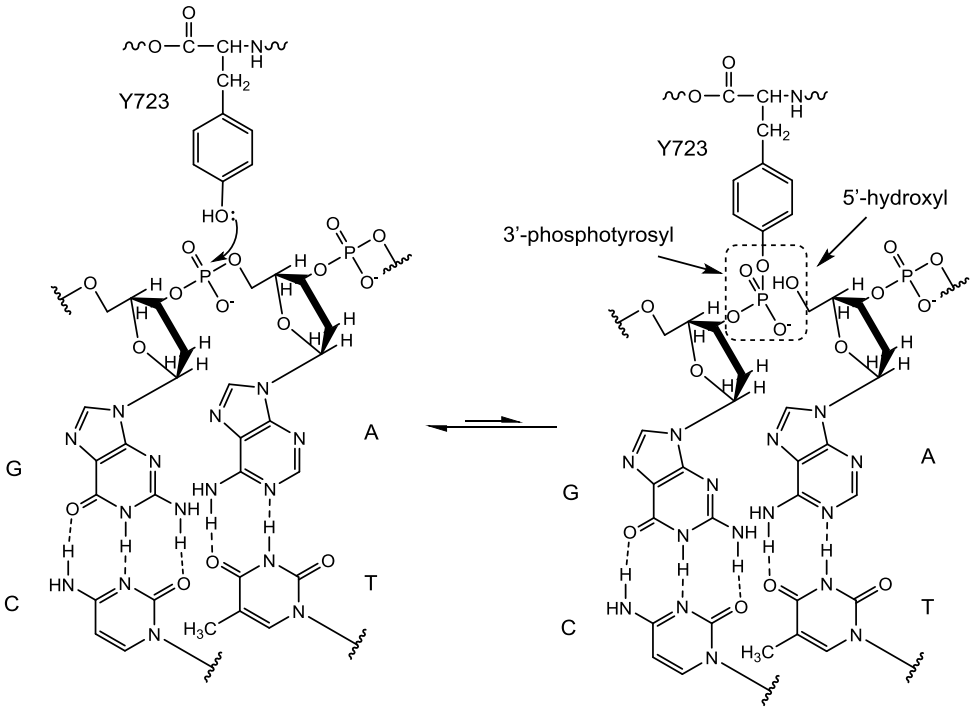

Figure 1-12 A schematic diagram depicting the formation of single-strand nick on DNA
The equilibrium favors the intact strand (the left form in the figure)

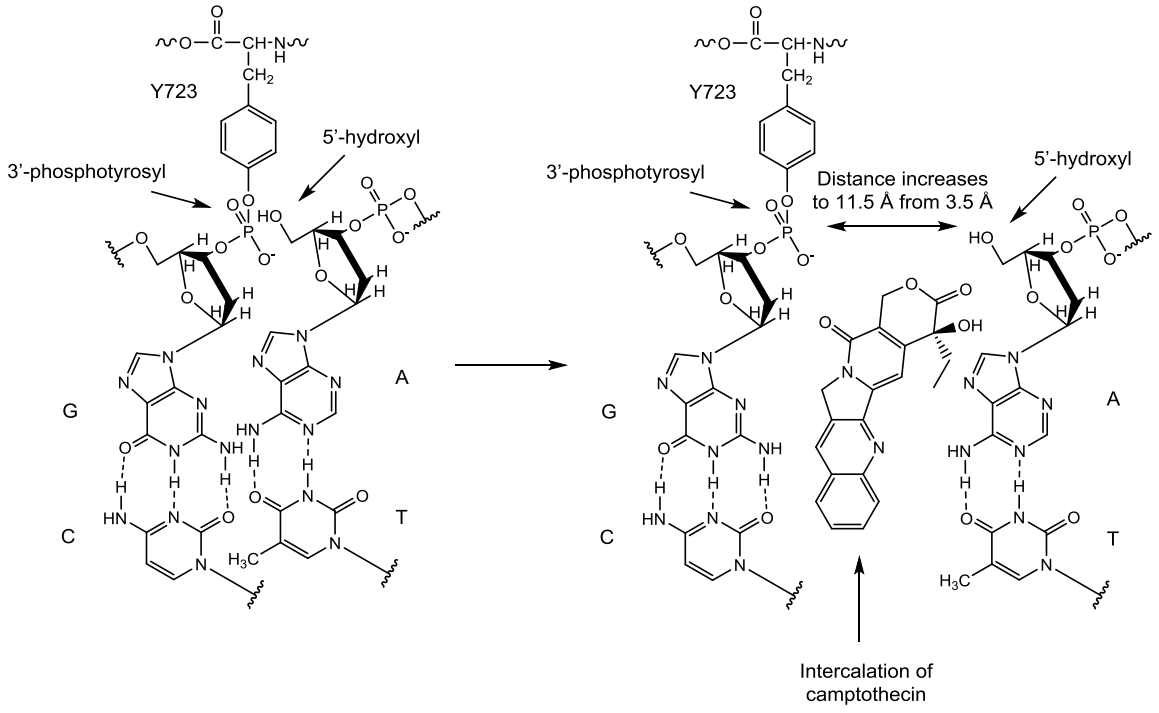

Figure 1-13 A schematic diagram depicting the intercalation of camptothecin in top1-DNA binary complex

Examination of X-ray crystal structure of the drug-stabilized ternary complex has revealed several key positions on the chemical structures of camptothecin and its derivatives. These positions are crucial to establishing strong interactions with both the DNA and enzyme. The overall planar structure of camptothecins is essential for the intercalation into DNA base pairs, and the N-1 on ring B, carbonyl at position 17 on ring D, and 20(*S*)-hydroxyl group on ring E are key moieties for the formation of hydrogen bonds with amino acid residues R364, N722 and D533 in human topoisomerase 1, respectively (Figure 1-14) [78]. The space accommodating the ring E is rather limited and therefore major structural modifications at positions around this ring are unlikely to be tolerated [75, 78].

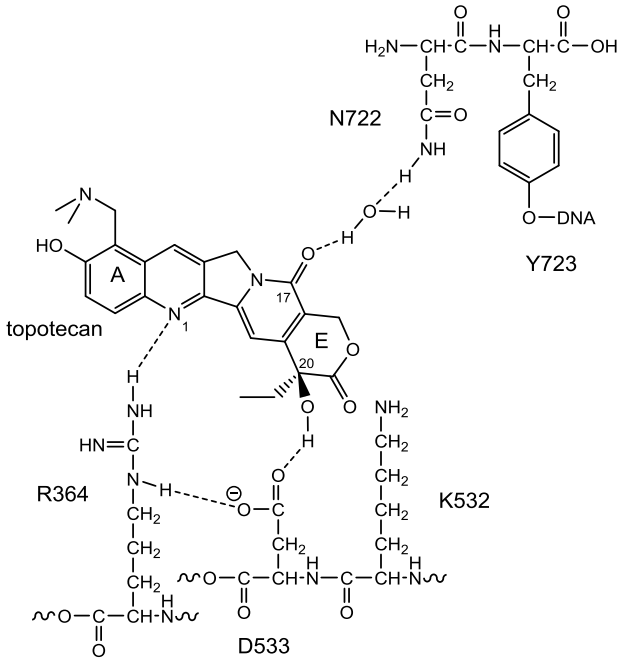

Figure 1-14 Hydrogen-bond network between topotecan and human topoisomerase 1

1.6.2 Inhibition of Hypoxia-Inducible Factor 1α

Hypoxia-inducible factors (HIFs) respond to the changes in oxygen levels, orchestrating the transcription of many proteins that are vital for the survival of hypoxic cancer cells [5]. In addition to the established topoisomerase inhibition, evidences also suggest that there is an additional mechanism of camptothecins' anticancer actions. Inhibition of hypoxia-inducible factor 1α (HIF-1α) has emerged as another component of camptothecins' antitumor mechanism. About a decade ago, three camptothecin analogues, including topotecan, were suggested as inhibitors of HIF-1 [76]; irinotecan also exhibited inhibitory effects on HIF-1α on nude mice implanted with colon cancer cells [80]. The affirmed HIF-1α inhibiting effects spurred researchers to resolve the mechanism of camptothecin-associated HIF-1α inhibition, and some results have been achieved recently.

Exerting the physiological function of HIF requires the formation of an HIF heterodimer by joining an HIF-1β subunit and HIF-α subunit. HIF-1β subunits are stably expressed in normal tissues; the expression rate of HIF-α subunits, however, is maintained low and accelerated only under oxygen-deficient state [5]. There are three isoforms of HIF-α subunits such as HIF-1α, HIF-2α and HIF-3α; only the accumulation of HIF-1α is mentioned to be reduced by camptothecins. The ternary complex of topoisomerase 1, camptothecin and DNA has displayed ability to elevate the amount of several microRNAs (miRNA), among which miR-17-5p and miR-155 are relevant to the translation of HIF-1α [77]. miRNA can bind with the messenger RNA (mRNA) and repress the translation from mRNA to corresponding proteins. Details about this process are unclear yet; hypothetical mechanisms include: inducing mRNA degradation, shortening mRNA's poly(A) tail, or impeding the movement of ribosomes [81].

1.6.3 Developing Hypoxia-Activated Camptothecins

Topotecan and SN-38, the active metabolite of irinotecan, were selected as parent drugs for hypoxia-activated camptothecins (Figure 1-15). Topotecan and irinotecan were both approved by the U.S. Food and Drug Administration in 1996 [74]. Experience in prescribing and studying these two camptothecins has accrued for nearly 20 years. With abundant clinical and academic data available, it is safe and rational to develop their hypoxia-activated versions. Furthermore, a dual cytotoxic effect on hypoxic tumor cells is expected to be exerted by topotecan and SN-38 due to their anti-HIF profile. As for the design of their hypoxia-activated versions, the fragmentation-activating strategy is preferred, as it generates approved drugs that are well-studied. Modifications on 10-positions should be able to effectively inactivate topotecan and SN-38. For example the installation of a bipiperidine-carboxylate group in irinotecan makes this prodrug 1,000-fold less active than its non-substituted metabolite SN-38 [74].

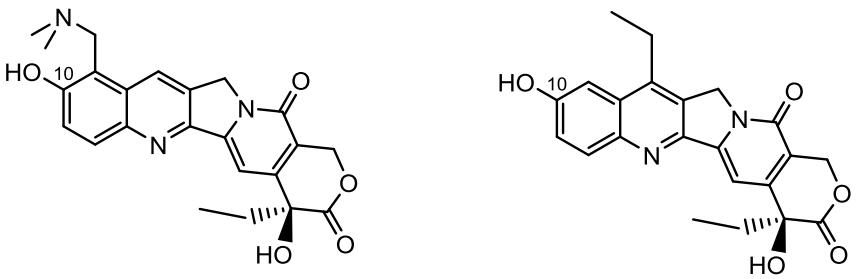

Figure 1-15 Structures of topotecan and SN-38

2 Arming SN-38 with Hypoxia-Activating Triggers

Three different nitrobenzyl groups (2-, 3-, and 4-substituted) were selected as triggers for hypoxia-activated topotecan and SN-38. Reactions exploiting a variety of alkylating agents such as mesylates, bromides and alkylating method such as Mitsunobu condition were conducted to synthesize these prodrugs. Unfortunately, despite all the attempts made, derivatives of topotecan could not be synthesized. Three nitrobenzyl SN-38 have been successfully obtained with good yields (Figure 2-1).

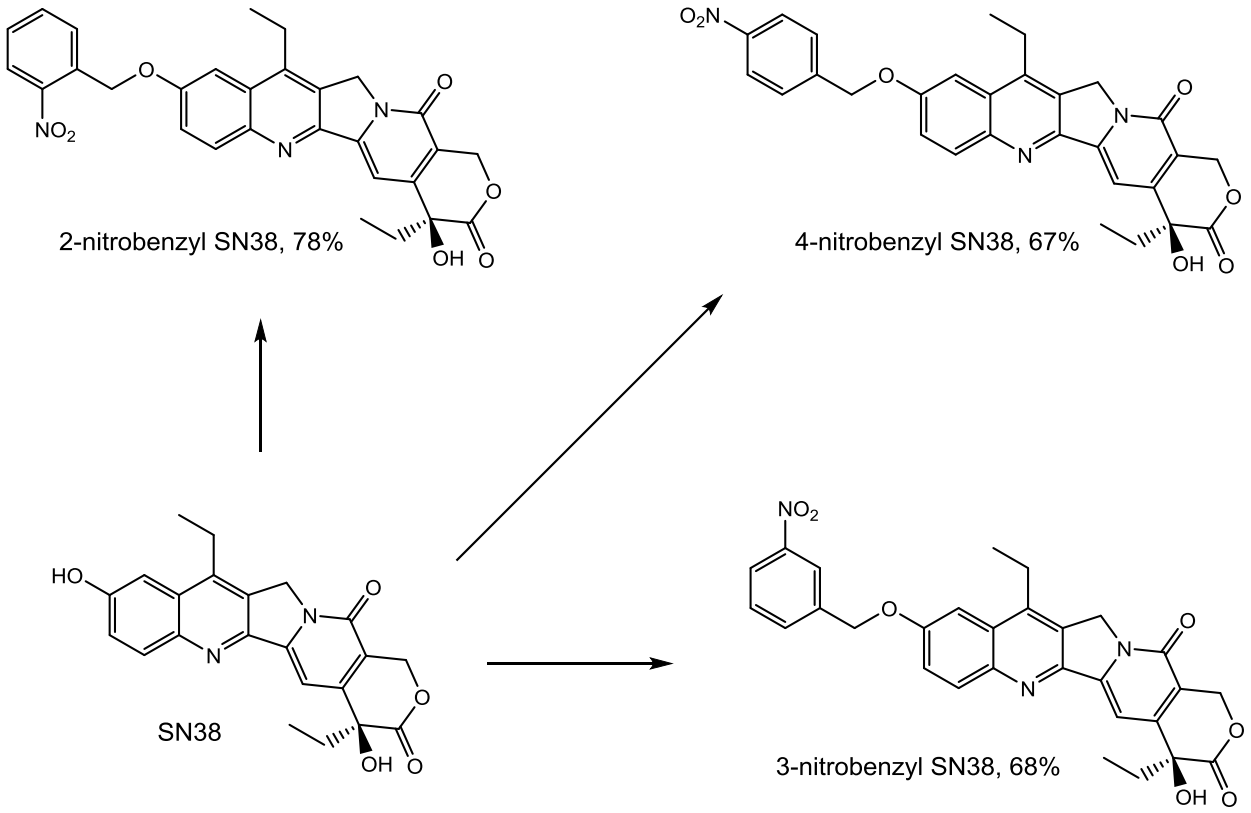

Figure 2-1 Structures of derivatives of SN-38

2.1 Syntheses and Characterizations

2.1.1 General Information

^{1}H and ^{13}C nuclear magnetic resonance (NMR) spectra were recorded on a Bruker 400 MHz spectrometer (400 and 101 MHz, respectively) using DMSO-d_6 (Merck KGaA, Germany) as solvent with tetramethylsilane (TMS) as an internal standard. Liquid chromatography-mass spectrometry (LC-MS) analyses were performed on a Shimadzu LC-MS spectrometer. SN-38 (7-ethyl-10-hydroxylcamptothecin, purity 95%+) was purchased from Ark Pharm, Inc., USA. 1,8-Diazabicyclo[5.4.0]undec-7-ene (DBU); 2-, 3- and 4-nitrobenzyl bromides were purchased from Sigma-Aldrich. Organic solvents were ordered from BDH, VWR Analytical unless specified otherwise. All chemicals were used without further purification unless otherwise indicated.

2.1.2 Characterization of SN-38

^{1}H NMR (400 MHz, DMSO) δ 10.28 (s, 1H), 8.02 (d, J = 8.9 Hz, 1H), 7.47 – 7.34 (m, 2H), 7.25 (s, 1H), 6.47 (s, 1H), 5.51 – 5.34 (s, 2H), 5.26 (s, 2H), 3.08 (q, J = 7.5 Hz, 2H), 1.94 – 1.75 (m, 2H), 1.30 (t, J = 7.6 Hz, 3H), 0.88 (t, J = 7.3 Hz, 3H). ^{13}C NMR (101 MHz, DMSO) δ 172.98, 157.32, 157.19, 150.53, 149.32, 146.91, 144.12, 143.21, 132.02, 128.66, 128.45, 122.84, 118.47, 105.25, 96.24, 72.87, 65.73, 49.91, 30.75, 22.74, 13.80, 8.21. ESI-MS(+) *m/z* (% relative intensity, [ion]): 393.20 (100, $[M + H]^+$), 434.25 (58.64, $[M + H + CH_3CN]^+$).

2.1.3 Synthesis and Characterization of 2-Nitrobenzyl SN-38

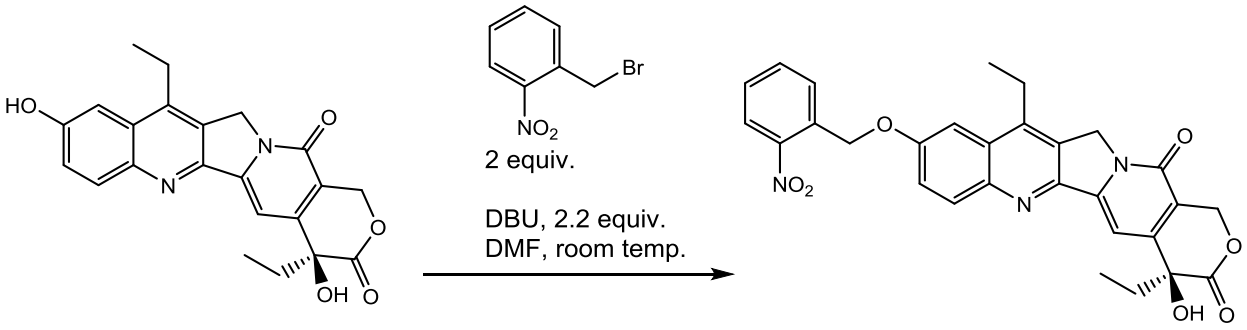

SN-38 (0.0941 g, 0.24 mmol) was added into a round bottom flask (10 mL) with a magnetic stirring bar. Dimethylformamide (DMF, 2.0 mL, anhydrous, Sigma-Aldrich) and DBU (80 µL, 0.54 mmol) were then added, and the mixture was sonicated until SN-38 was dissolved. The dissolved SN-38 was then stirred on a stirring plate and purged with argon flow for 20 min. 2-Nitrobenzyl bromide (0.1149 g, 0.53 mmol) was dissolved in 0.75 mL anhydrous DMF and then added slowly (over 30 min) into SN-38 with a syringe. The mixture was allowed to stir at room temperature (22 ^{o}C) for 6 hours. The resulted yellow solid was separated by centrifuging and washed with acetone (2 mL x 5). Residual acetone was then evaporated under vacuum to give 2-nitrobenzyl SN-38 as a yellow powder (0.0986 g, 78%). ^{1}H NMR (400 MHz, DMSO) δ 8.21 – 8.06 (m, 2H), 7.89 (d, *J* = 7.5 Hz, 1H), 7.81 (t, *J* = 7.3 Hz, 1H), 7.66 (t, *J* = 7.4 Hz, 1H), 7.59 (d, *J* = 7.7 Hz, 2H), 7.28 (s, 1H), 6.52 (s, 1H), 5.72 (s, 2H), 5.43 (s, 2H), 5.31 (s, 2H), 3.17 (q, *J* = 7.4 Hz, 2H), 1.87 (m, *J* = 14.2, 6.9 Hz, 2H), 1.23 (t, *J* =7.5 Hz, 3H), 0.88 (t, *J* = 7.3 Hz, 3H). ^{13}C NMR (101 MHz, DMSO) δ 173.00, 157.31, 157.14, 150.53, 150.44, 148.31, 146.70, 145.10, 144.48, 134.41, 132.14, 130.25, 129.92, 129.00, 128.19, 125.34, 122.73, 118.84, 104.64, 99.98, 96.56, 72.86, 67.32, 65.71, 50.02, 30.68, 22.67, 13.86, 8.23. ESI-MS(+) *m/z* (% relative intensity, [ion]): 528.20 (100, $[M + H]^{+}$), 569,25 (57.55, $[M + H + CH_3CN]^{+}$).

2.1.4 Synthesis and Characterization of 3-Nitrobenzyl SN-38

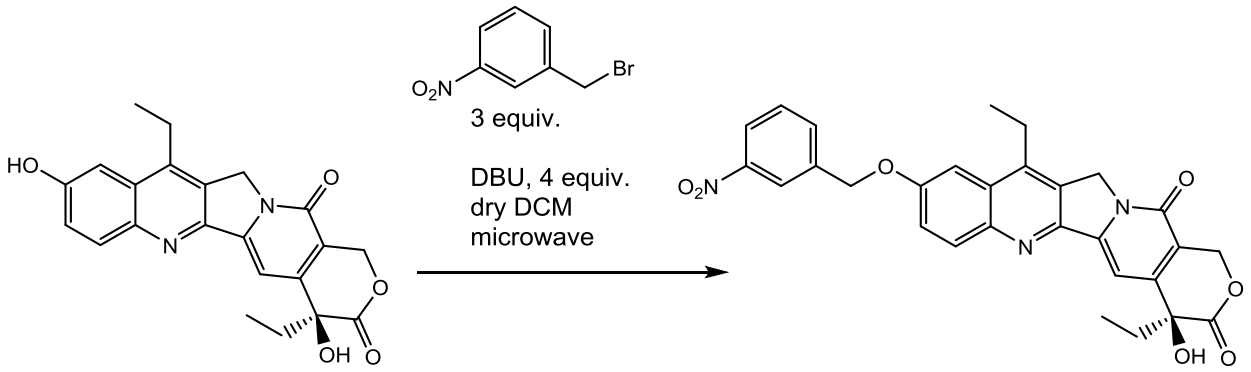

This synthesis was conducted on a microwave synthesizer (Discover®SP W/Activent, CEM, USA). To a microwave reaction vessel (10 mL) were added SN-38 (0.0241 g, 0.061 mmol), dry dichloromethane (DCM, 4 mL, dried over molecular sieves overnight), DBU (36 µL, 0.24 mmol) and 3-nitrobenzyl bromide (0.0375 g, 0.17 mmol). The reaction vessel was then sealed and placed in the microwave synthesizer. The reaction was conducted under dynamic mode, 66 ^{o}C, PowerMax mode (simultaneous air cooling, model of microwave synthesizer: Discover®SP W/Activent, CEM, USA), max power 200 W, max pressure 300 psi, for 10 min. The reaction mixture was then purified with silica gel column chromatography on a CombiFlash® Rf 200 purification system, Teledyne Isco, USA, with ethyl acetate in hexane from 0% to 100% (3-nitrobenzyl SN-38 was eluted out with 100% ethyl acetate). Residual solvent was evaporated under vacuum to give 3-nitrobenzyl SN-38 as a yellow powder (0.0216 g, 67%). ^{1}H NMR (400 MHz, DMSO) δ 8.46 (s, 1H), 8.24 (dd, *J* = 8.2, 1.5 Hz, 1H), 8.17 – 8.08 (m, 1H), 8.04 (d, *J* = 7.8 Hz, 1H), 7.75 (t, *J* = 7.9 Hz, 1H), 7.64 (dd, *J* = 6.7, 3.1 Hz, 2H), 7.28 (s, 1H), 6.53 (s, 1H), 5.55 (s, 2H), 5.43 (s, 2H), 5.31 (s, 2H), 3.20 (q, *J* = 7.3 Hz, 2H), 1.96 – 1.77 (m, 2H), 1.24 (t, *J* = 7.6 Hz, 3H), 0.88 (t, *J* = 7.3 Hz, 3H). ^{13}C NMR (101 MHz, DMSO) δ 173.00, 157.27, 157.19, 150.50, 150.27, 148.33, 146.67, 145.00, 144.40, 139.54, 134.75, 132.05, 130.66, 128.89, 128.15, 123.37, 122.96, 122.79, 118.78, 104.35, 96.54, 72.86, 68.88, 65.71, 49.97, 30.69, 22.67, 13.85,

8.23. ESI-MS(+) *m/z* (% relative intensity, [ion]): 528.20 (100, $[M + H]^+$), 569,30 (69.21, $[M + H + CH_3CN]^+$).

2.1.5 Synthesis and Characterization of 4-Nitrobenzyl SN-38

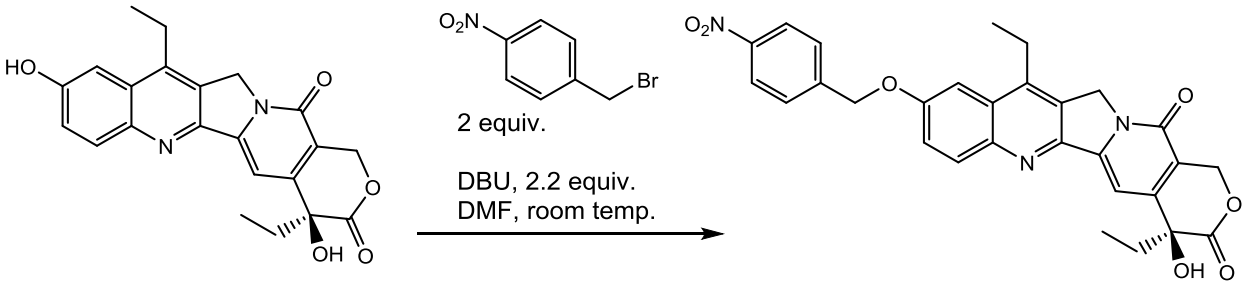

SN-38 (0.0936 g, 0.24 mmol) was added into a round bottom flask (10 mL) with a magnetic stirring bar. Dimethylformamide (DMF, 2.0 mL, anhydrous, Sigma-Aldrich) and DBU (80 µL, 0.54 mmol) were then added, and the mixture was sonicated until SN-38 was dissolved. The dissolved SN-38 was then stirred on a stirring plate and purged with argon flow for 20 min. 4-Nitrobenzyl bromide (0.1187 g, 0.55 mmol) was dissolved in 0.75 mL anhydrous DMF and then added slowly (over 30 min) into SN-38 with a syringe. The mixture was allowed to stir at room temperature (22 ^oC) for 6 hours. The resulted yellow solid was separated by centrifuging and washed with acetone (2 mL x 5). Residual acetone was then evaporated under vacuum to give 4-nitrobenzyl SN-38 as a yellow powder (0.0864 g, 68%). ^1H NMR (400 MHz, DMSO) δ 8.35 – 8.26 (m, 2H), 8.13 (d, *J* = 9.1 Hz, 1H), 7.85 (d, *J* = 8.8 Hz, 2H), 7.63 (dt, *J* = 5.7, 2.6 Hz, 2H), 7.28 (s, 1H), 6.53 (s, 1H), 5.56 (s, 2H), 5.43 (s, 2H), 5.31 (s, 2H), 3.18 (q, *J* = 7.4 Hz, 2H), 1.87 (m, *J* = 14.0, 7.1 Hz, 2H), 1.25 (t, *J* = 7.6 Hz, 3H), 0.88 (t, *J* = 7.3 Hz, 3H). ^{13}C NMR (101 MHz, DMSO) δ 172.98, 157.33, 157.25, 150.54, 150.39, 147.61, 146.72, 145.10, 145.08, 144.49, 132.12, 128.98, 128.23, 124.16, 122.94, 118.84, 104.55, 96.56, 72.87, 71.45, 69.07, 65.74, 50.00,

30.76, 22.68, 13.89, 8.21. ESI-MS(+) *m/z* (% relative intensity, [ion]): 528.25 (100, $[M + H]^+$), 569,30 (92.39, $[M + H + CH_3CN]^+$).

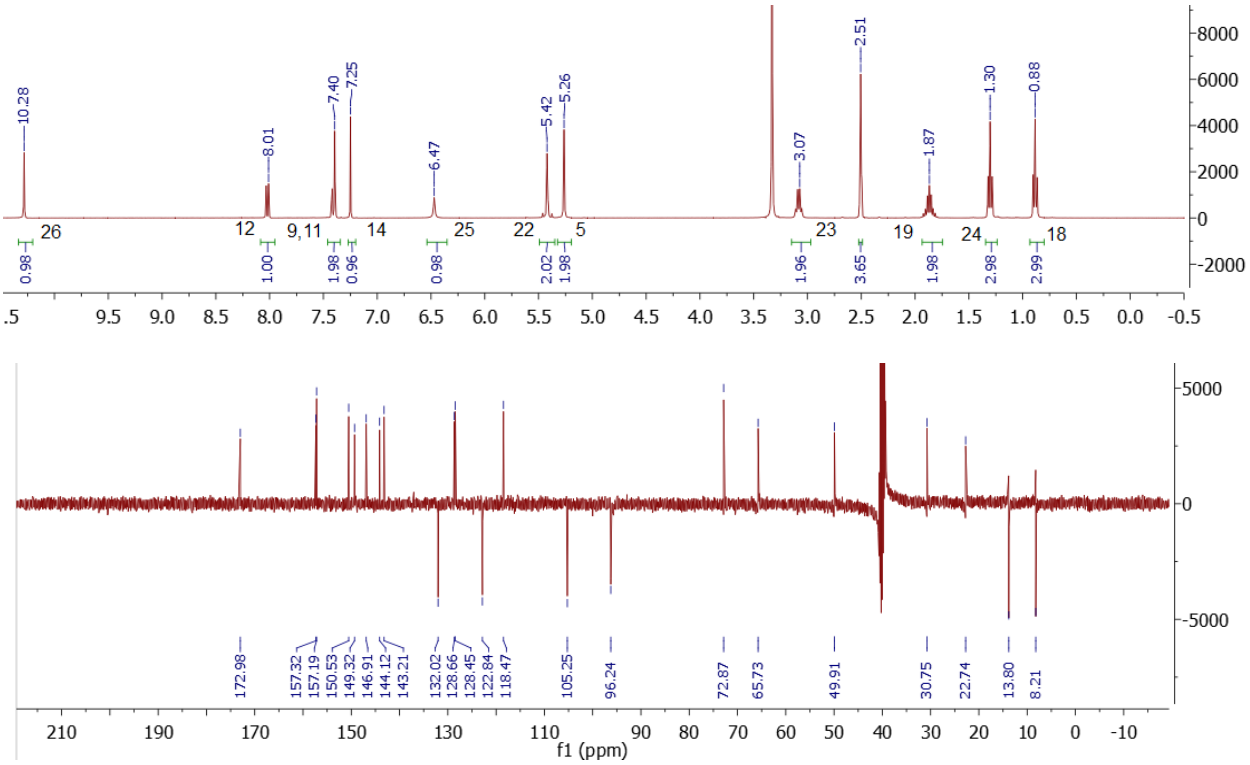

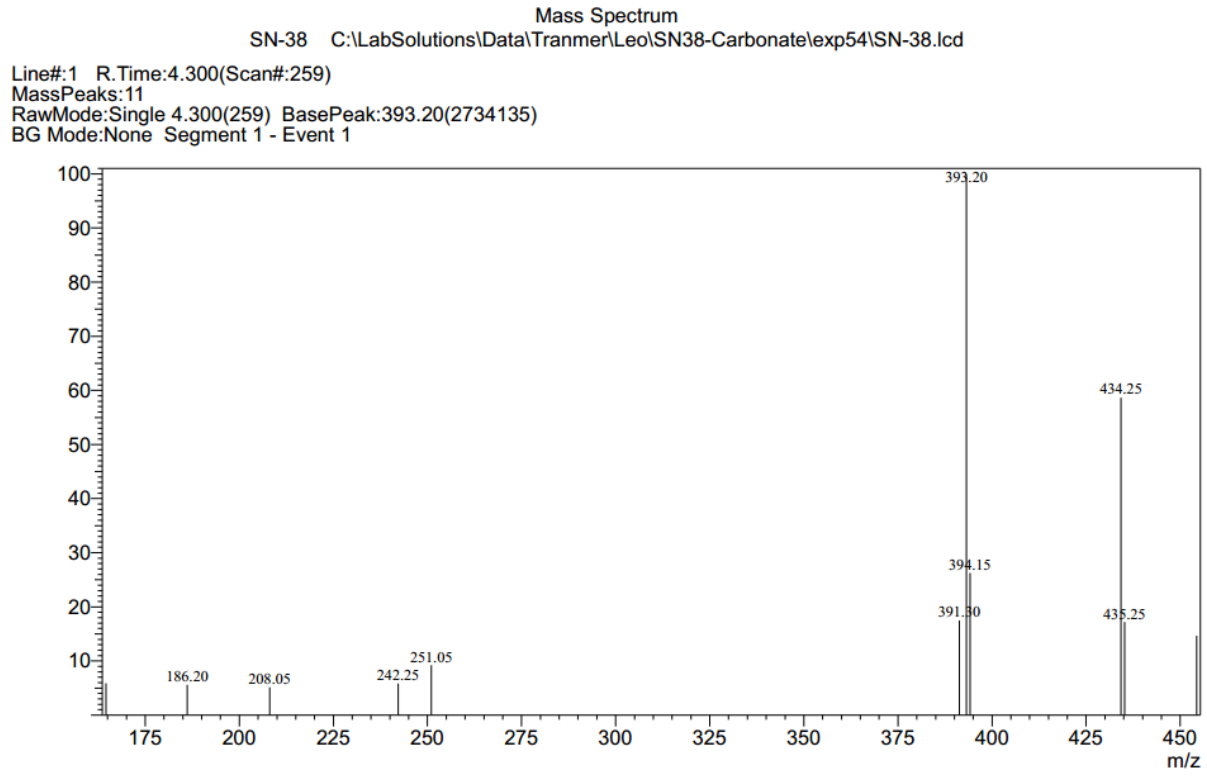

Figure 2-2 ^{1}H NMR, ^{13}C NMR, and MS spectra of SN-38

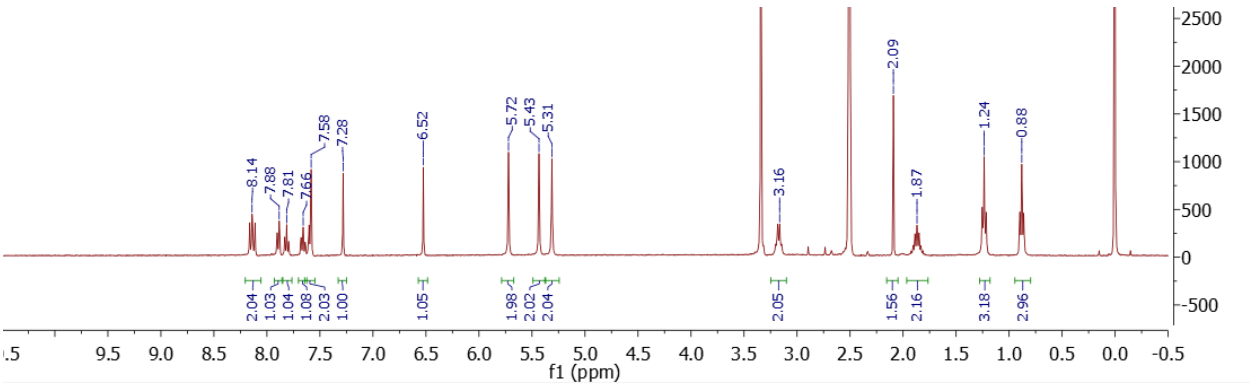

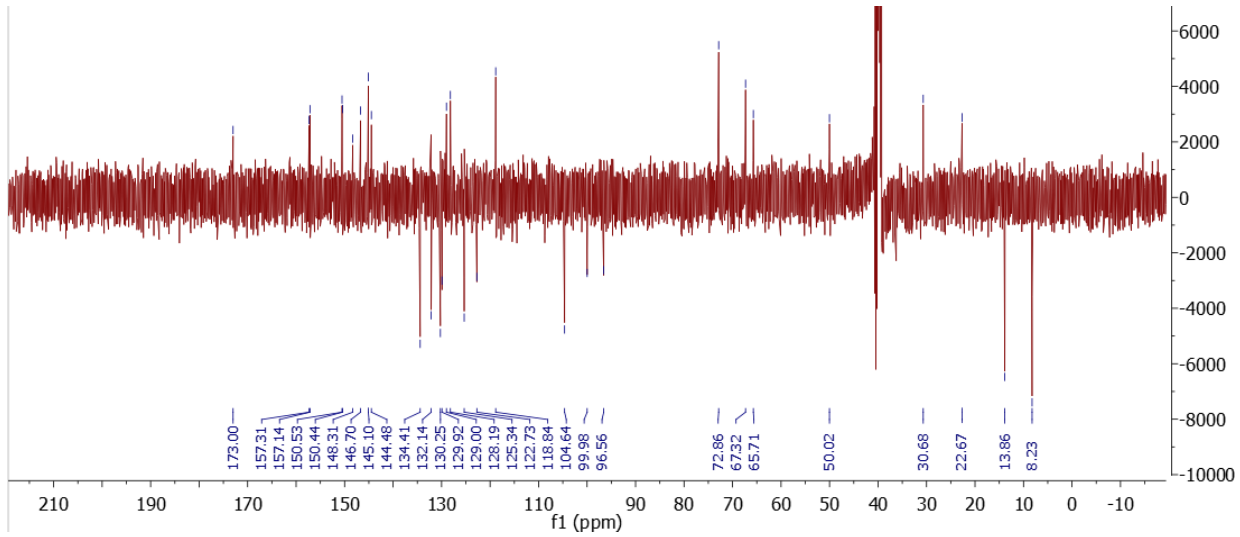

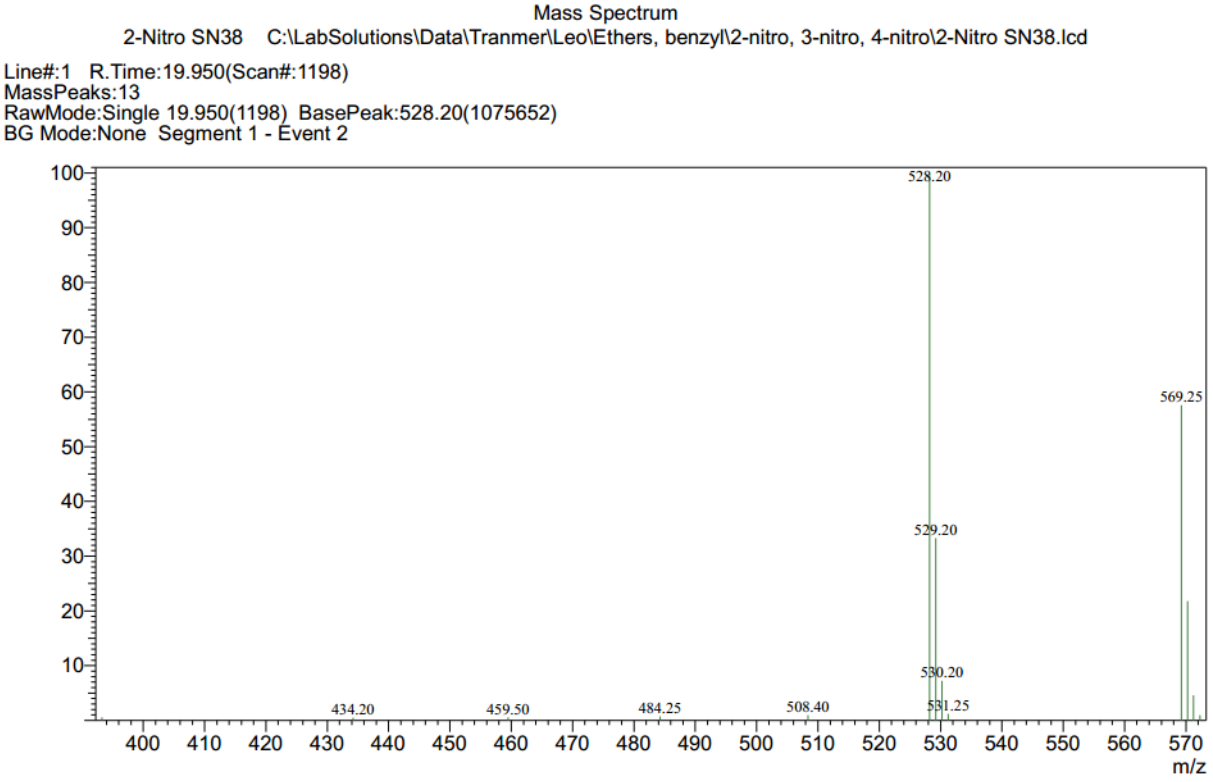

Figure 2-3 ^{1}H NMR, ^{13}C NMR, and MS spectra of 2-nitrobenzyl SN-38

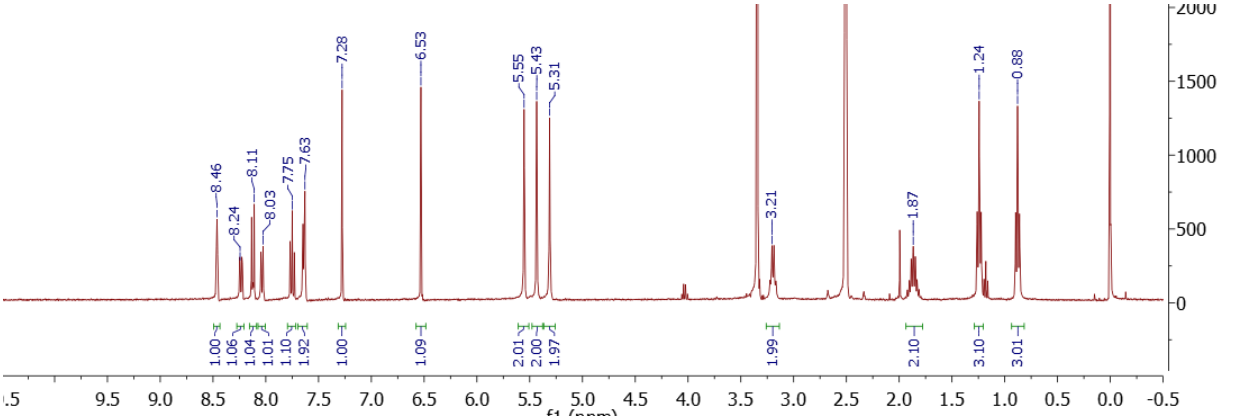
8.46
8.24
8.11
8.03
7.75
7.63
7.28
6.53
5.55
5.43
5.31
3.21
1.87
1.24
0.88
1.00
1.06
1.04
1.01
1.10
1.92
1.00
1.09
2.01
2.00
1.97
1.99
2.10
3.10
3.01
f1 (ppm)

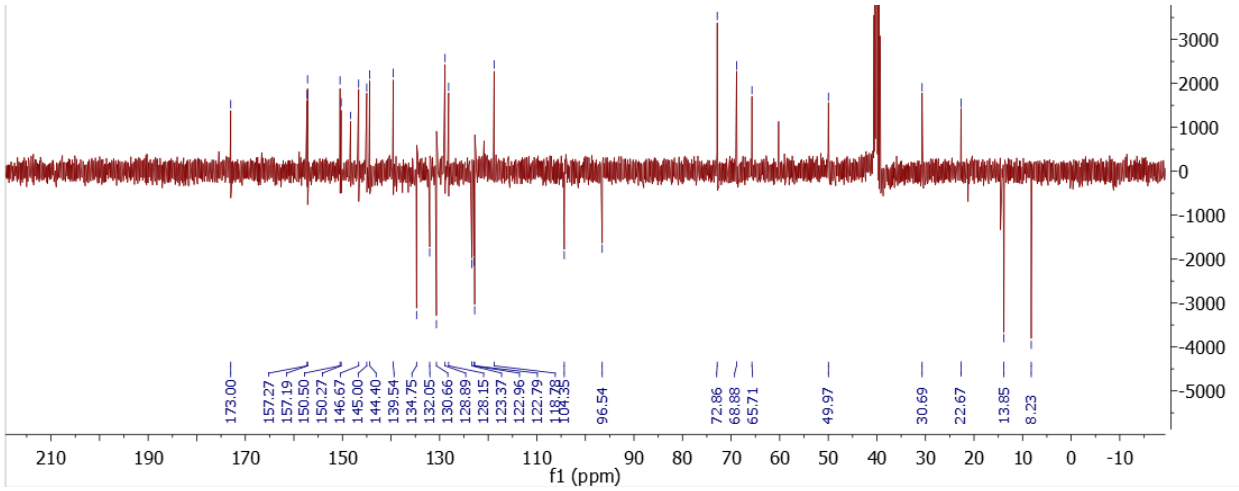
173.00
157.27
157.19
150.50
150.27
146.67
145.00
144.40
139.54
134.75
132.05
130.66
128.89
128.15
123.37
122.96
122.79
118.78
104.38
96.54
72.86
68.88
65.71
49.97
30.69
22.67
13.85
8.23
f1 (ppm)

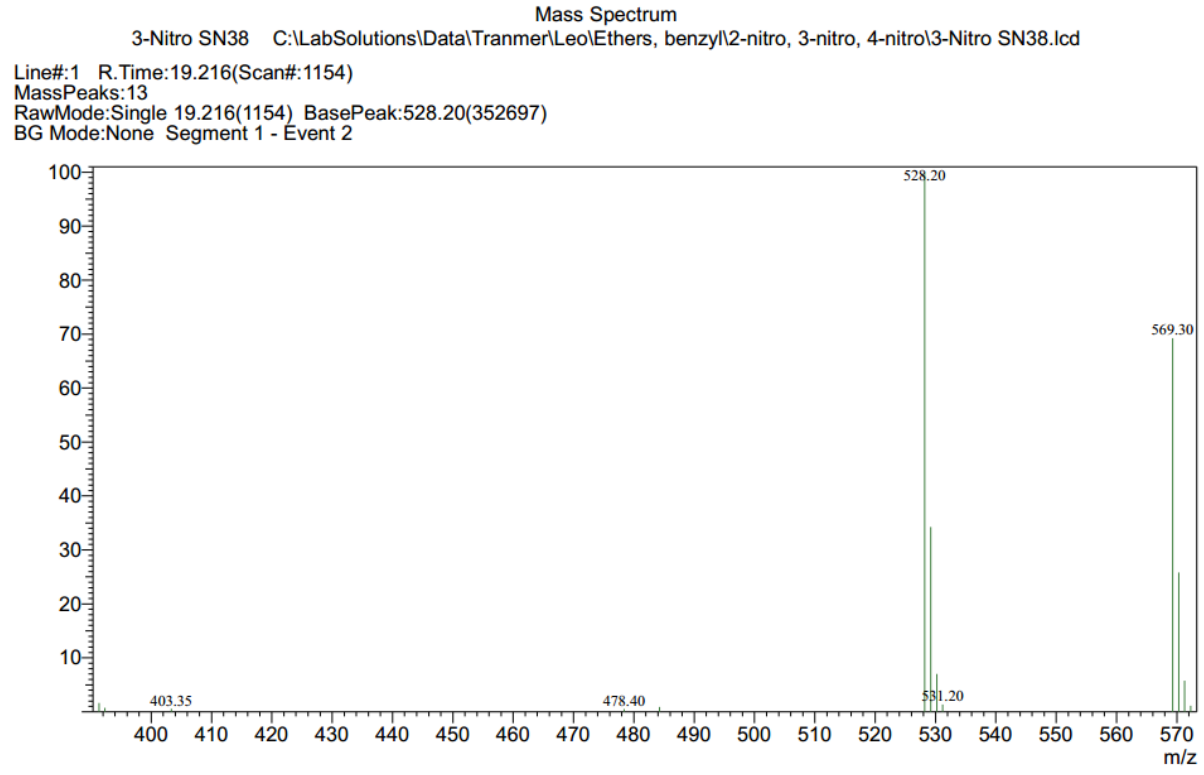

Figure 2-4 ^{1}H NMR, ^{13}C NMR, and MS spectra of 3-nitrobenzyl SN-38

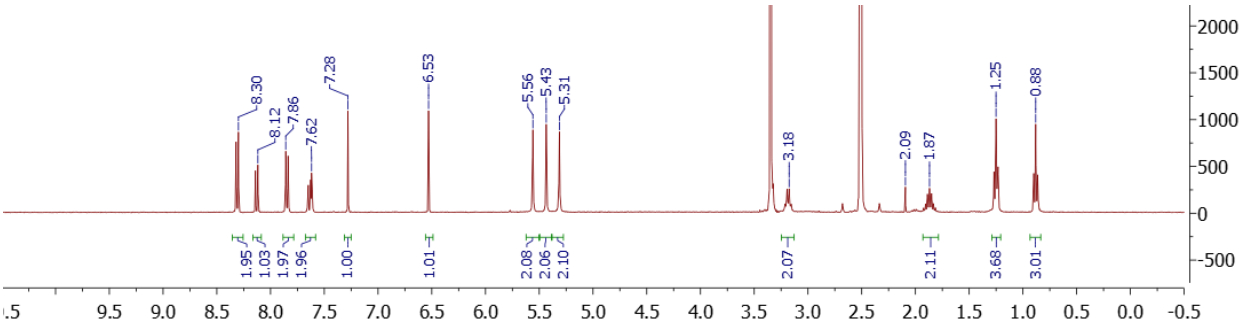

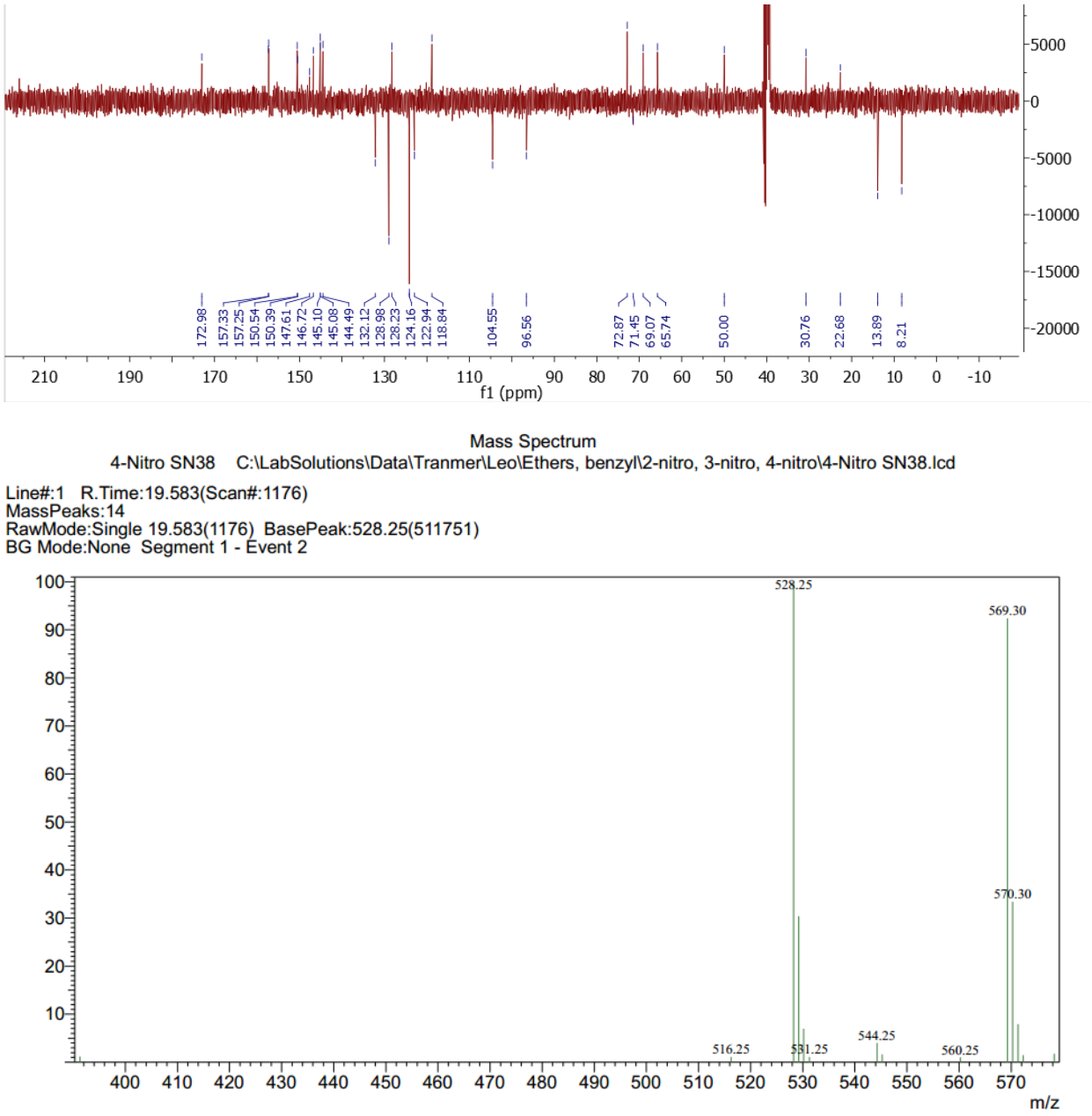

Figure 2-5 ^{1}H NMR, ^{13}C NMR, and MS spectra of 4-nitrobenzyl SN-38

2.2 Topoisomerase I Inhibitory Assay and Cell Viability Assay

The obtained 2-nitrobenzyl SN-38 and 4-nitrobenzyl SN-38 have been tested in topoisomerase 1 inhibitory assay and cell viability assay to investigate their manner of action. The majority of

operations of topoisomerase 1 inhibitory assay and cell viability assay were kindly performed by Mr. Xing Wu with methods established by Dr. Brian B. Hasinoff's group [82, 83].

2.2.1 Experimental Section

Topoisomerase 1 Inhibitory Assay: The recombinant human topoisomerase 1, pBR322 DNA, and assay buffer were from TopoGEN, Inc. Each 20 μL of assay mixture contained 50 ng of pBR322 DNA, 0.5 units of topoisomerase 1 (except the mixture for the control lane "no top1") and tested drugs of indicated final concentrations. The order of addition was assay buffer, DNA, drug, and then topoisomerase 1. After incubation at 37°C in assay buffer for 30 min, the reaction was terminated with 0.5% (v/v) SDS and 25 mM Na_2EDTA. Electrophoresis was carried out at 8 V/cm for 1 h on a plate of agarose gel (1.2%, w/v). The gel plate was then stained with ethidium bromide for 20 min and immersed in water for 24 h to elute the drugs (SN-38 and its derivatives emit strong fluorescence under UV light, impairing the quality of image). The gel plate was then visualized by UV light, and the emitted fluorescence was recorded on an Alpha Innotech (San Leandro, CA) Fluorochem 8900 imaging system equipped with a 365-nm UV illuminator and a charge-coupled device camera.

Cell Viability Assay: Human leukemia K562 cells were obtained from the American Type Culture Collection and maintained as suspension cultures in Dulbecco's modified Eagle's medium (Invitrogen) containing 4 mM L-glutamine and supplemented with 20 mM HEPES (Sigma-Aldrich, St. Louis, MO), 10% fetal calf serum (Invitrogen), 100 units/mL penicillin G, and 100 μg/mL streptomycin in an atmosphere of 5% CO_2 and 95% air at 37°C, pH 7.4. Cells in exponential growth were harvested and seeded with 1150 cells/well in 96-well microtiter plates

(100 μL/well). Tested drugs were dissolved in dimethyl sulfoxide (Fisher Scientific) with 11 different concentrations to construct the dose-response curves and were added to give a final volume of 200 μL/well. Each drug was tested in two adjacent lanes of wells. The final concentration of dimethyl sulfoxide did not exceed 0.5% (v/v), and it was an amount that had no detectable effect on cell growth. The cells were incubated with tested drugs for 48 h and then assayed with MTS on a spectrophotometer (SpectraMax 190, Molecular Devices). Values of half maximal inhibitory concentrations (IC_{50}) were obtained by fitting the average absorbance-concentration data of two lanes to a four-parameter logistic equation (SigmaPlot, Jandel, San Rafael CA).

2.2.2 Results

Topoisomerase 1 Inhibitory Assay: Effects of SN-38, 2-nitrobenzyl SN-38 and 4-nitrobenzyl SN-38 on the ability of topoisomerase 1 to relax pBR322 DNA are shown on the color-reversed fluorescent image of a plate of gel stained with ethidium bromide (Figure 2-6). In this gel the supercoiled DNA (SC) was located below the relaxed DNA (RLX). The relaxed DNA was not well resolved from the nicked circular DNA (NC). All lanes except the lane "no top1" contained topoisomerase 1. No drug was added to the lane "Ctr". The known topoisomerase 1 inhibitor SN-38 (20 and 100 μM) inhibited the DNA-supercoil-relaxing activity of topoisomerase 1; 2-nitrobenzyl SN-38 did not show inhibitory effect at tested concentrations (5 and 20 μM); whereas 4-nitrobenzyl SN-38 did not show inhibitory effect at 5 μM but did so at the higher concentration (20 μM).

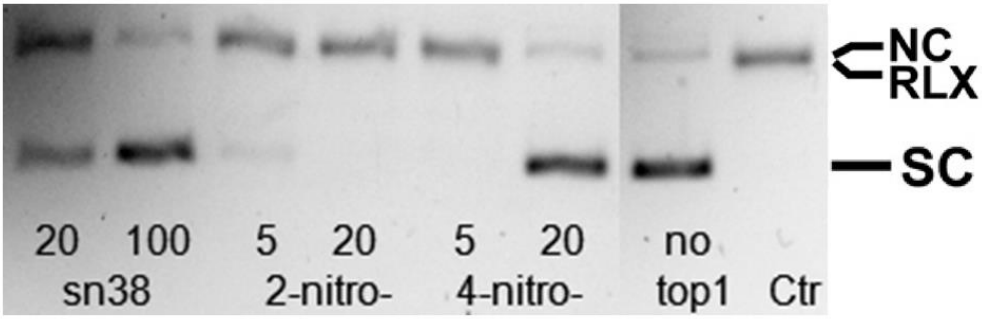

Figure 2-6 Effects of SN-38, 2-nitrobenzyl SN-38 and 4-nitrobenzyl SN-38 on the ability of topoisomerase 1 to relax pBR322 DNA
NC, nicked circular DNA; RLX, relaxed DNA; SC, supercoiled DNA; "sn38", "2-nitro-" and "4-nitro-" denote the tested drugs SN-38, 2-nitrobenzyl SN-38 and 4-nitrobenzyl SN-38, respectively; numbers indicate the final concentration [μM] of tested drug in the assay mixture applied to the lanes above; all lanes except the lane "no top1" contained topoisomerase 1; no drug was added to the lane "Ctr"

Cell Viability Assay: SN-38 and three nitrobenzyl derivatives of SN-38 were tested on human leukemia K562 cells to evaluate their effects on cell growth. The half maximal inhibitory concentrations (IC_{50}) of SN-38, 2-, 3- and 4-nitrobenzyl SN-38 were 3.0, 25.9, 12.2 and 58.0 nM, respectively (Figure 2-7). All nitrobenzyl derivatives of SN-38 appeared to be less toxic to K562 cells than SN-38, by around 8, 4 and 19 folds, respectively.

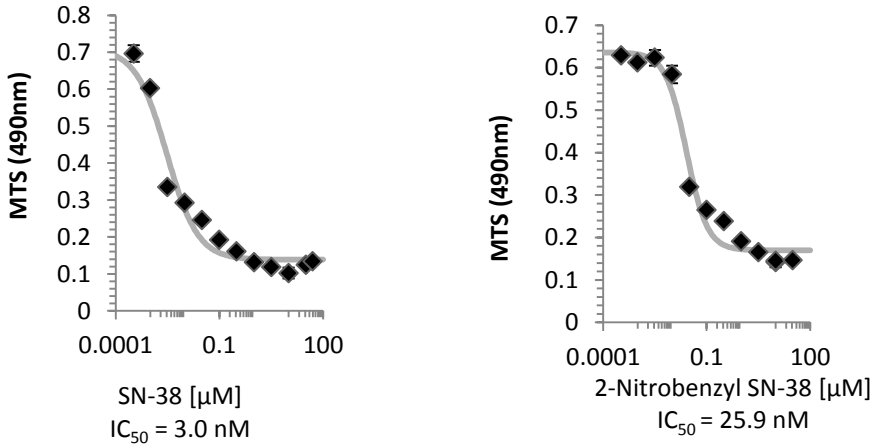

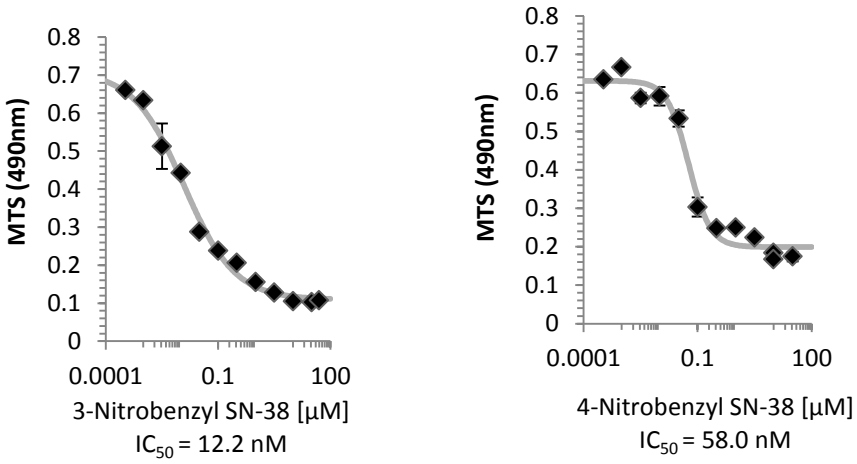

Figure 2-7 Dose response curves and values of IC_{50}/nM of SN-38, 2-nitrobenzyl SN-38, 3-nitrobenzyl SN-38 and 4-nitrobenzyl SN-38

2.2.3 Discussion

The result of cell viability tests suggests that these three nitrobenzyl derivatives of SN-38 have less toxicity to K562 cells. This property meets the principle of prodrug design that requires a prodrug to be less toxic than its parent drug. This result has also supported the hypothesis that a bulky trigger installed on the 10-OH can reduce the anticancer activity/toxicity of SN-38. The most effective deactivating trigger shown in this result is the 4-nitrobenzyl group, which leads to a compound 19-fold less toxic than SN-38. However, these triggers are much less effective in deactivating SN-38 than the dipiperidine group of irinotecan, which lowers down the activity of SN-38 by 1000 fold [74]. Bulkier triggers need to be designed to reduce the toxicity further (see the section "Directions of Future Work" below).

An interesting observation has been noticed when comparing the Top1 inhibitory assay with cell viability assay. 2-Nitrobenzyl SN-38 did not show Top1 inhibitory effect at concentration 20 μM but the 4-nitro version did; however, the 2-nitro version appeared to be more toxic to K562 cells

than 4-nitrobenzyl SN-38 (IC_{50} of 2- and 4-nitrobenzyl SN-38 are 25.9 and 58.0 nM, respectively). A possible explanation to this observation is that 2-nitrobenzyl may be more effective than 4-nitrobenzyl SN-38 in certain Top1-inhibition-independent cytotoxic mechanisms, such as HIF-1 inhibition. Further study is warranted to validate this speculation.

2.3 Cyclic Voltammetry

The electrochemical properties of 2-, 3-, and 4-nitrobenzyl SN38s have been measured by cyclic voltammetry. Dr. David Herbert kindly offered help with cyclic voltammetry measurements.

2.3.1 Experimental Section

Cyclic voltammetry was performed on dimethyl sulfoxide (DMSO, Fisher Scientific) solutions of 1 mM SN-38 derivatives with 0.1 M lithium perchlorate ($LiClO_4$, battery grade, dry, 99.99% trace metals basis, Sigma-Aldrich) as supporting electrolyte. Argon was bubbled through DMSO for at least 10 min to remove residual oxygen in solvent before taking measurements. Measurements were taken with a CHI760C electrochemical workstation connected with a three-electrode cell (a platinum wire as an auxiliary electrode, an Ag/Ag^+ electrode as a reference electrode and a glass working electrode). Ferrocene (1 mM, Sigma-Aldrich) was used as an internal standard reference of reduction potential. The scan rate of each test shown was 250 mV/s.

2.3.2 Results

Important parameters of a cyclic voltammogram were collected in Table 1, wherein E_{pa}^{Ag} (E_{pc}^{Ag}) is anodic (cathodic) peak potential of derivatives of SN-38 against Ag/Ag^+ electrode; i_{pa} (i_{pc}) is

anodic (cathodic) peak current of SN-38 derivatives; i_{pa}/i_{pc} is peak current ratio; $E_{pa}{}^{Ag}$(Fc) [$E_{pc}{}^{Ag}$(Fc)] is the anodic [cathodic] peak potential of the internal standard ferrocene against Ag/Ag^+ electrode.

The half-wave potential ($E_{1/2}$) (also known as formal reduction potential, $E^{o'}$ or E_f) is:

$$E_{1/2} = \frac{E_{pa} + E_{pc}}{2} \quad (1)$$

$E_{1/2}{}^{Ag}$ [$E_{1/2}{}^{Ag}$(Fc)] is the half-wave potential of SN-38 derivatives [ferrocene] against Ag/Ag^+ electrode. $E_{1/2}{}^{Fc}$ is the half-wave potential of SN-38 derivatives against the internal standard ferrocene/ferrocenium (Fc/Fc^+) redox couple:

$$E_{1/2}^{Fc} = E_{1/2}^{Ag} - E_{1/2}^{Ag}(Fc) \quad (2)$$

$E_{1/2}{}^{NHE}$ is the value against normal hydrogen electrode (NHE) for the convenience of comparing data with those in literature, which is converted via:

$$E_{1/2}^{NHE} = E_{1/2}^{Fc} + 450\ mV + 250\ mV \quad (3)$$

where the +450 mV[84] is to relate a potential to saturated calomel electrode (SCE) and the +250 mV[85] is to convert a value against SCE to a value against NHE. {Please note: despite the author's best effort, exact reference potentials for conversions could not be found. Therefore, $E_{1/2}$

(450 mV[84]) of ferrocene in DMSO with 0.1 M tetrabutylammonium perchlorate as supporting electrolyte vs SCE ($E_{1/2}^{Fc}$ DMSO/[NBu_4][ClO_4]) was used for conversion of $E_{1/2}^{Fc}$ DMSO/$LiClO_4$ (1 M lithium perchlorate as supporting electrolyte). For the same reason, the conversion constant between SCE and NHE in acetonitrile (250 mV [85]) was used for converting data acquired in DMSO}

Table 1: Results of cyclic voltammetry of SN-38 derivatives

	E_{pa}^{Ag}/mV	i_{pa}/µA	E_{pc}^{Ag}/mV	i_{pc}/µA	E_{pa}^{Ag}(Fc)/mV	E_{pc}^{Ag}(Fc)/mV
2-Nitrobenzyl SN38	-948	5.81	-1033	-9.86	427	514
3-Nitrobenzyl SN38	-929	5.55	-1043	-10.14	405	509
4-Nitrobenzyl SN38	-882	4.17	-1055	-11.97	427	504

Cont'd	i_{pa}/i_{pc}	$E_{1/2}^{Ag}$(Fc)/mV	$E_{1/2}^{Ag}$/mV	$E_{1/2}^{Fc}$/mV	$E_{1/2}^{NHE}$/mV
	0.589	471	-991	-1461	-761
	0.548	457	-986	-1443	-743
	0.348	466	-969	-1434	-734

2.3.3 Discussion

The validity of reduction potentials obtained in this work was checked by comparing the values with cyclic voltammetry data of similar compounds in literature. The reported values of $E_{1/2}^{Fc}$ of

nitrobenzene and 4-nitrotoluene are -1492 mV and −1547 mV[86], respectively, which are comparable to the values (-1434 ~ -1461 mV) obtained in this work. However, care should be taken when drawing conclusions by comparing values measured by a different method such as pulse radiolysis, as there seems to be an inconsistency between the values. For example, the $E_{1/2}^{NHE}$ of nitrobenzene (-792 mV) converted from $E_{1/2}^{Fc}$ with eq. 3 does not match the E^1 (-486 mV vs. NHE) measured by pulse radiolysis[29].

As hypoxia-activated prodrugs (HAPs) are to be reduced by one-electron reductases, the redox properties of these enzymes are important references when consider the suitability of designed compounds as HAPs. Previous studies have revealed four possibly involved one-electron reductases such as NADPH:cytochrome P450 oxidoreductase (POR)[45], methionine synthase reductase (MTRR)[38], NADPH dependent diflavin oxidoreductase 1 (NDOR)[53] and inducible nitric oxide synthase (iNOS)[54]. Substrates of these enzymes can receive an electron from a catalytic site containing flavin mononucleotide (FMN)[55]. Reduction potentials of the FMN group [semiquinone/hydroquinone] of NDOR1[56], POR[57], iNOS[58] and MTRR[59] are -305, -269, -245 and -227 mV, respectively. (vs. NHE, measured by potentiometric titration) These values are considerably higher than the $E_{1/2}^{NHE}$ (-761 ~ -734 mV) of three nitrobenzyl SN-38s. One might think these reductases could experience difficulty in reducing these compounds, if reduction potentials of enzymes and substrates are the only factor to consider. However, in physiological conditions, these reductases do not work at the standard state but with NAD(P)H as an electron donor[55]. In fact, the reduction potential (-407 mV) of the most advanced HAP, TH-302, is also lower than that of these enzymes. Further examination of these SN-38 derivatives in hypoxic tumor cells is warranted to investigate the process of activation.

Previous studies have suggested an empirical range of one-electron reduction potentials (E^1) for hypoxia-activated prodrugs as -400 to -200 mV[14, 15] or as a lower and narrower window between -450 and -300 mV[16, 22] (vs. NHE). However, very few data of reduction potentials are available for individual HAPs that are currently being studied. Browsing through publications has only resulted data of two nitroaromatic HAPs, TH-302 and KS119 (Figure 2-8). The one-electron reduction potentials E^1 of the currently most advanced prodrug TH-302 is -407 mV vs. NHE (obtained by pulse radiolysis)[30]. The half-wave reduction potential $E_{1/2}^{Ag}$ of KS119 is -415 and -575 mV vs. Ag/Ag^+ (measured on a racemic mixture by differential pulse polarography)[48]; authors of the reference did not provide an explanation of the origin of the two different values. Half-wave reduction potentials of the three tested SN-38 derivatives ($E_{1/2}^{NHE}$ -761 ~ -734 mV, $E_{1/2}^{Ag}$ -991 ~ -969 mV) appear to lower than that of TH-302 and KS119. However, as mentioned before, whether comparison can be drawn across values obtained by different methods is unclear yet. Assuming that these data are comparable, the higher reduction potential of TH-302 probably originates from the more electronegative nitrogen heteroatoms in the ring system. Some researchers also suggest the protonation on the unsubstituted nitrogen of imidazole as an important origin of further elevated potential in physiological conditions[20]. As for KS119, the unexpected high reduction potential is probably derived from the electron-withdrawing effect of the carbamyl on benzylic carbon. These potential-elevating features can be included in the design of next generation of hypoxia-activated SN-38, if activating tests in hypoxic tumor cells suggests reduction potentials of SN-38 derivatives are not high enough.

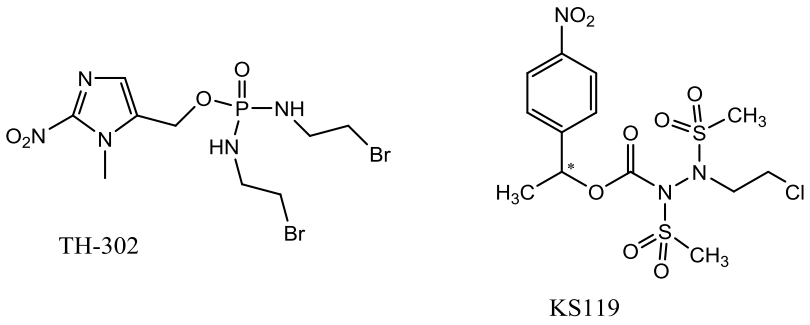

Figure 2-8 Structures of TH-302 and KS119

Finally, the reversibility of the initial one-electron reduction of the HAP-activating process, i.e. the inter-transition between a nitro prodrug and its radical anion in the presence of normal level of oxygen, is a key element in the formation of the futile cycle under normoxic conditions, imparting the hypoxic selectivity to HAPs (Figure 2-9). The peak current ratio i_{pa}/i_{pc} can provide some information on the extent of reversibility. The closer to 1 the ratio, the more reversible under the testing condition the reaction is. The peak current ratio of 2-, 3-, and 4-nitrobenzyl SN-38s are 0.589, 0.548 and 0.348, respectively, indicating the reductions are quasi-reversible under the testing condition. There may be an inverse relationship between i_{pa}/i_{pc} and the distance from the nitro substituent to the benzylic carbon atom, i.e. from *ortho*- to *para*- substitution, as the *para*-nitro group is supposed to be the most "exposed" and therefore the most subject to the influence of external factors. External factors such as type of solvent, rate of scan, amount of water in solvent can also influence the value of i_{pa}/i_{pc}.

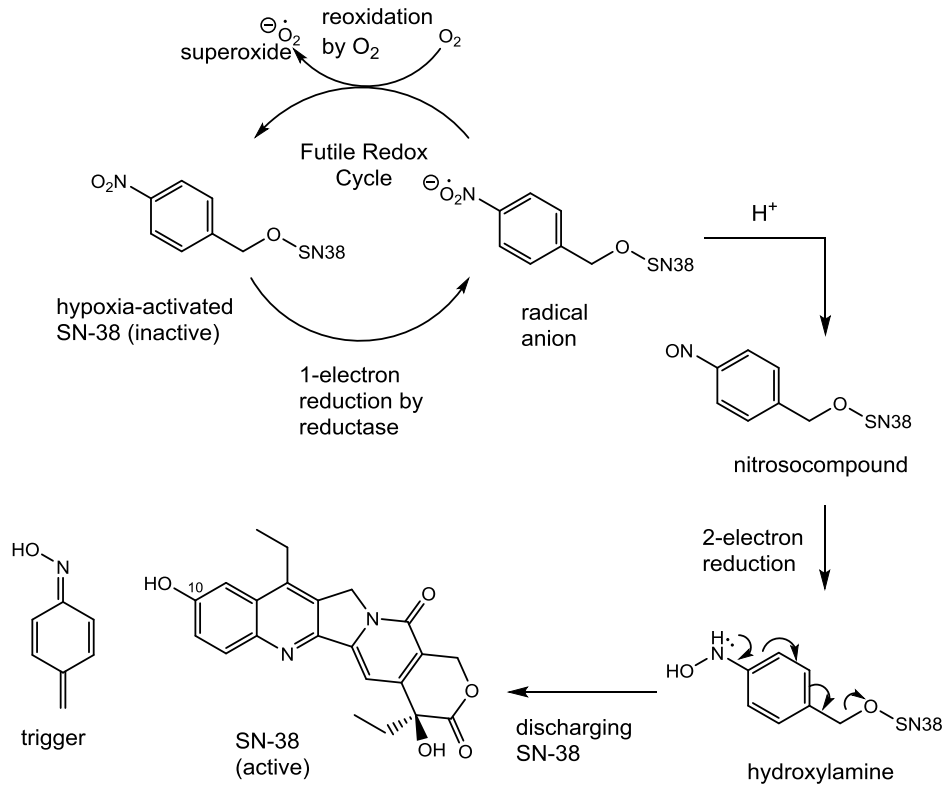

Figure 2-9 Proposed mechanism of activation of hypoxia-activated SN-38

3 Directions of Future Work

As discussed in previous sections, the next generation of hypoxia-activated SN-38s requires elevation in reduction potential and further decrease in toxicity. To fulfill these requirements, two new derivatives have been designed and their synthetic methods have been suggested. The first design is a modification of the nitroimidazole trigger of TH-302 (Figure 3-1). Although TH-302 did not meet its endpoints in two phase 3 clinical trials, it did leave its nitroimidazole group as a legacy of excellent hypoxia-activated trigger. Nitroimidazole has an intrinsically higher reduction potential than a nitrobenzene, probably due to the stronger electronegativity of

nitrogen atoms in an imidazole than that of carbon atoms in a benzene ring. Some researchers also suggest the protonation on the unsubstituted nitrogen of imidazole as an important origin of further elevated potential in physiological conditions[20]. The bulky benzyl group on nitroimidazole trigger for SN-38 can potentially be made by modifying methods from references [87, 88].

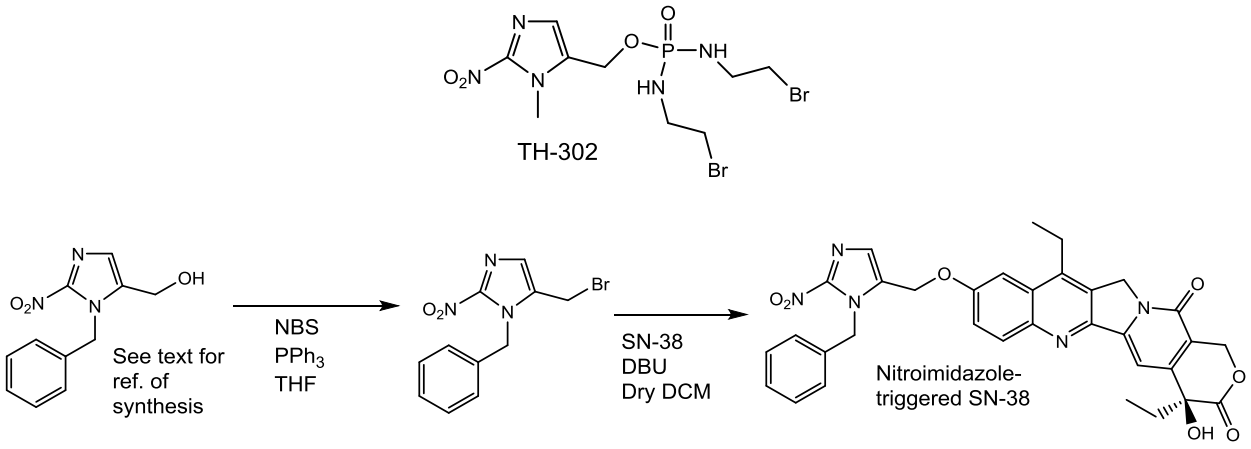

Figure 3-1 Structures of TH-302 and nitroimidazole-triggered SN-38 with synthetic route

Another way to elevate reduction potential is using triggers with multiple electron-withdrawing groups, which is the strategy adopted by the second design. A substituted dinitrobenzene is selected as the trigger (Figure 3-2). In the suggested synthesis, the commercially available 2,4-dinitro-3-bromotoluene can be coupled with styrene via Heck reaction, resulting a rigid substituted stilbene. The rigidity of stilbene may be beneficial for effective deactivation of SN-38.

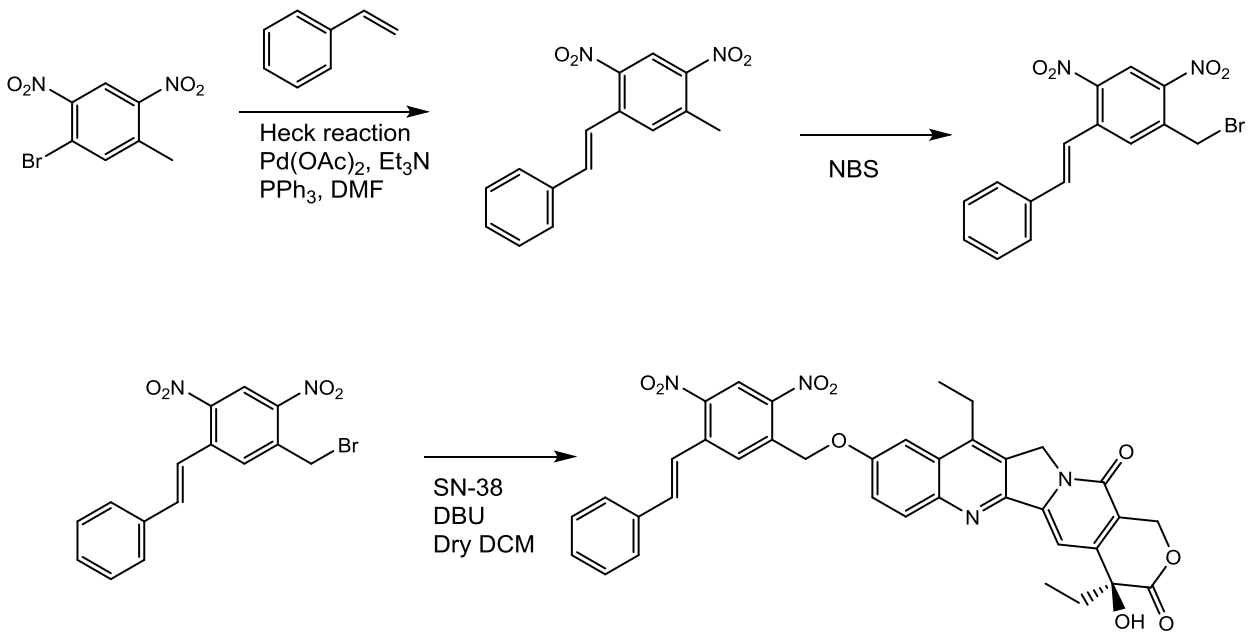

Figure 3-2 Structure and synthetic route of dinitrobenzene-triggered SN-38

4 Conclusion

2-, 3-, And 4-nitrobenzyl derivatives of SN-38 have been successfully synthesized with good yields (78%, 67% and 68%, respectively). Topoisomerase 1 inhibitory assay on 2- and 4-nitrobenzyl SN-38s and cell viability assay on 2-, 3- and 4-nitrobenzyl SN-38s have been performed. All three derivatives showed less toxicity on K562 cells, which meets the principle of prodrug design. However, bulkier triggers need to be designed and synthesized to further reduce the toxicity of prodrugs. The results of cyclic voltammetry suggest that the reduction of three nitrobenzyl SN-38s is partly reversible under the testing condition. This manner of reduction is not against the proposed mechanism of activation. Provided reduction potentials are comparable across methods of measurements, the values of these SN-38 derivatives appear to be lower than the reported values of other HAPs. Further examination of these SN-38 derivatives in hypoxic tumor cells is warranted to investigate the process of activation. If activating tests in hypoxic

tumor cells suggests that reduction potentials of SN-38 derivatives are not high enough, some potential-elevating features can be included in the design of next generation of hypoxia-activated SN-38s. Two examples of the next generation of SN-38 prodrugs with bulkier and more electron-withdrawing triggers have been suggested. As an inhibitor of both topoisomerase 1 and HIF-1, SN-38 has a completely different anticancer mechanism than the DNA-alkylator TH-302, which did not meet endpoints in two phase 3 clinical trials. We hope our hypoxia-activated SN-38 with its different mechanism of action and the expected dual inhibitory effect on hypoxic tumor cells can bring a bright future to hypoxia-activated prodrugs.

References

[1] Höckel, M.; Vaupel, P., Tumor Hypoxia: Definitions and Current Clinical, Biologic, and Molecular Aspects. *J. Natl. Cancer Inst.* **2001,** *93* (4), 266–276.

[2] Vaupel, P.; Kallinowski, F.; Okunieff, P., Blood Flow, Oxygen and Nutrient Supply, and Metabolic Microenvironment of Human Tumors: A Review. *Cancer Res.* **1989,** *49* (23), 6449–6465.

[3] Giaccia, A. J., Hypoxic Stress Proteins: Survival of the Fittest. *Semin. Radiat. Oncol.* **1996,** *6* (1), 46–58.

[4] Cheng, K. C.; Loeb, L. A., Genomic Instability and Tumor Progression: Mechanistic Considerations. *Adv. Cancer Res.* **1993,** *60*, 121–156.

[5] Pouysségur, J.; Dayan, F.; Mazure, N. M., Hypoxia Signalling in Cancer and Approaches To Enforce Tumour Regression. *Nature* **2006,** *441*, 437–443.

[6] Mandriota, S. J.; Pepper, M. S., Regulation of Angiopoietin-2 mRNA Levels in Bovine Microvascular Endothelial Cells by Cytokines and Hypoxia. *Circul. Res.* **1998,** *83* (8), 852–859.

[7] Ikeda, E.; Achen, M. G.; Breier, G.; Risau, W., Hypoxia-Induced Transcriptional Activation and Increased mRNA Stability of Vascular Endothelial Growth Factor in C6 Glioma Cells. *J. Biol. Chem.* **1995,** *270* (34), 19761–19766.

[8] Höckel, M.; Schlenger, K.; Aral, B.; Mitze, M.; Schäffer, U.; Vaupel, P., Association between Tumor Hypoxia and Malignant Progression in Advanced Cancer of the Uterine Cervix. *Cancer Res.* **1996,** *56* (19), 4509–4515.

[9] Wilson, W. R.; Hay, M. P., Targeting Hypoxia in Cancer Therapy. *Nature Reviews Cancer* **2011,** *11*, 393–410.

[10] Cater, D. B.; Phillips, A. F., Measurement of Electrode Potentials in Living and Dead Tissues. *Nature* **1954,** *174*, 121–123.

[11] Jiang, J.; Auchinvole, C.; Fisher, K.; Campbell, C. J., Quantitative Measurement of Redox Potential in Hypoxic Cells Using SERS Nanosensors. *Nanoscale* **2014,** *6*, 12104–12110.

[12] Denny, W.; Wilson, W.; Hay, M., Recent Developments in the Design of Bioreductive Drugs. *Br. J. Cancer* **1996,** *74* (Suppl. XXVII), S32–S38.
[13] Siim, B. G.; Denny, W. A.; Wilson, W. R., Nitro Reduction as an Electronic Switch for Bioreductive Drug Activation. *Oncol. Res.* **1997,** *9*, 357–369.
[14] Wardman, P., Electron Transfer and Oxidative Stress as Key Factors in the Design of Drugs Selectively Active in Hypoxia. *Curr. Med. Chem.* **2001,** *8*, 739–761.
[15] Denny, W. A.; Wilson, W. R., Considerations for the Design of Nitrophenyl Mustards as Agents with Selective Toxicity for Hypoxic Tumor Cells. *J. Med. Chem.* **1986,** *29*, 879–887.
[16] Mason, R. P.; Holtzman, J. L., The Role of Catalytic Superoxide Formation in the O_2 Inhibition of Nitroreductase. *Biochem. Biophys. Res. Commun.* **1975,** *67* (4), 1267–1274.
[17] Benov, L., How Superoxide Radical Damages the Cell. *Protoplasma* **2001,** *217*, 33–36.
[18] Fridovich, I., Superoxide Dismutases. *Adv. Enzymol. Relat. Areas Mol. Biol.* **1986,** *58*, 61–97.
[19] Kovacic, P.; Kassel, M. A.; Feinberg, B. A.; Corbett, M. D.; Mcclelland, R. A., Reduction Potentials in Relation to Physiological Activities of Benzenoid and Heterocyclic Nitroso Compounds: Comparison with the Nitro Precursors. *Bioorg. Chem.* **1990,** *18* (3), 265–275.
[20] Wardman, P., Some reactions and properties of nitro radical-anions important in biology and medicine. *Environ. Health Perspect.* **1985,** *64*, 309-320.
[21] Beveridge, A. J.; Williams, M.; Jenkins, T. C., Calculation of One-Electron Reduction Potentials for Nitroheterocyclic Hypoxia-Selective Agents. *J. Chem. Soc., Faraday Trans.* **1996,** *92* (5), 763–768.
[22] Denny, W. A.; Wilson, W. R., Bioreducible Mustards: a Paradigm for Hypoxia-Selective Prodrugs of Diffusible Cytotoxins (HPDCs). *Cancer Metastasis Rev.* **1993,** *12*, 135–151.
[23] Allalunis, M. J.; Chapman, J. D.; Turner, A. R., Identification of a Hypoxic Population of Bone Marrow Cells. *Int. J. Radiat. Oncol. Biol. Phys.* **1983,** *9* (2), 227–232.
[24] Nombela-Arrieta, C.; Pivarnik, G.; Winkel, B.; Canty, K. J.; Harley, B.; Mahoney, J. E.; Park, S.-Y.; Lu, J.; Protopopov, A.; Silberstein, L. E., Quantitative Imaging of Haematopoietic Stem and Progenitor Cell Localization and Hypoxic Status in the Bone Marrow Microenvironment. *Nat. Cell Biol.* **2013,** *15*, 533–543.
[25] Parmar, K.; Mauch, P.; Vergilio, J.-A.; Sackstein, R.; Down, J. D., Distribution of Hematopoietic Stem Cells in the Bone Marrow According to Regional Hypoxia. *Proc. Natl. Acad. Sci. U. S. A.* **2007,** *104* (13), 5431–5436.
[26] Parliament, M. B.; Wiebe, L. I.; Franko, A. J., Nitroimidazole Adducts as Markers for Tissue Hypoxia: Mechanistic Studies in Aerobic Normal Tissues and Tumour Cells. *Br. J. Cancer* **1992,** *66*, 1103–1108.
[27] Lee, A. E.; Wilson, W. R., Hypoxia-Dependent Retinal Toxicity of Bioreductive Anticancer Prodrugs in Mice. *Toxicol. Appl. Pharmacol.* **2000,** *163* (1), 50–59.
[28] Evans, S. M.; Schrlau, A. E.; Chalian, A. A.; Zhang, P.; Koch, C. J., Oxygen Levels in Normal and Previously Irradiated Human Skin as Assessed by EF5 Binding. *J. Invest. Dermatol.* **2006,** *126*, 2596–2606.
[29] Wardman, P., Reduction Potentials of One-Electron Couples Involving Free Radicals in Aqueous Solution. *J. Phys. Chem. Ref. Data* **1989,** *18* (4), 1637–1755.
[30] Meng, F.; Evans, J. W.; Bhupathi, D.; Banica, M.; Lan, L.; Lorente, G.; Duan, J.-X.; Cai, X.; Mowday, A. M.; Guise, C. P.; Maroz, A.; Anderson, R. F.; Patterson, A. V.; Stachelek, G. C.; Glazer, P. M.; Matteucci, M. D.; Hart, C. P., Molecular and Cellular Pharmacology of the Hypoxia-Activated Prodrug TH-302. *Mol. Cancer Ther.* **2012,** *11* (3), 740–751.
[31] Pruijn, F. B.; Patel, K.; Hay, M. P.; Wilson, W. R.; Hicks, K. O., Prediction of Tumour Tissue Diffusion Coefficients of Hypoxia-Activated Prodrugs from Physicochemical Parameters. *Aust. J. Chem.* **2008,** *61* (9), 687–693.

[32] Foehrenbacher, A.; Patel, K.; Abbattista, M. R.; Guise, C. P.; Secomb, T. W.; Wilson, W. R.; Hicks, K. O., The Role of Bystander Effects in the Antitumor Activity of the Hypoxia-Activated Prodrug PR-104. *Front. Oncol.* **2013,** *3*, article 263.

[33] Chowdhury, G.; Junnotula, V.; Daniels, J. S.; Greenberg, M. M.; Gates, K. S., DNA Strand Damage Product Analysis Provides Evidence that the Tumor Cell-Specific Cytotoxin Tirapazamine Produces Hydroxyl Radical and Acts as a Surrogate for O_2. *J. Am. Chem. Soc.* **2007,** *129* (42), 12870–12877.

[34] Shinde, S. S.; Hay, M. P.; Patterson, A. V.; Denny, W. A.; Anderson, R. F., Spin Trapping of Radicals Other Than the •OH Radical upon Reduction of the Anticancer Agent Tirapazamine by Cytochrome P450 Reductase. *J. Am. Chem. Soc.* **2009,** *131* (40), 14220–14221.

[35] Wilson, W. R.; Hicks, K. O.; Pullen, S. M.; Ferry, D. M.; Helsby, N. A.; Patterson, A. V., Bystander Effects of Bioreductive Drugs: Potential for Exploiting Pathological Tumor Hypoxia with Dinitrobenzamide Mustards. *Radiat. Res.* **2007,** *167*, 625–636.

[36] Patterson, A. V.; Ferry, D. M.; Edmunds, S. J.; Gu, Y.; Singleton, R. S.; Patel, K.; Pullen, S. M.; Hicks, K. O.; Syddall, S. P.; Atwell, G. J.; Yang, S.; Denny, W. A.; Wilson, W. R., Mechanism of Action and Preclinical Antitumor Activity of the Novel Hypoxia-Activated DNA Cross-Linking Agent PR-104. *Clin. Cancer. Res.* **2007,** *13*, 3922–3932.

[37] Guise, C. P.; Wang, A. T.; Theil, A.; Bridewell, D. J.; Wilson, W. R.; Patterson, A. V., Identification of Human Reductases that Activate the Dinitrobenzamide Mustard Prodrug PR-104A: A Role for NADPH:Cytochrome P450 Oxidoreductase under Hypoxia. *Biochem. Pharmacol.* **2007,** *74*, 810–820.

[38] Guise, C. P.; Abbattista, M. R.; Tipparaju, S. R.; Lambie, N. K.; Su, J.; Li, D.; Wilson, W. R.; Dachs, G. U.; Patterson, A. V., Diflavin Oxidoreductases Activate the Bioreductive Prodrug PR-104A under Hypoxia. *Mol. Pharmacol.* **2012,** *81* (1), 31–40.

[39] Hunter, F. W.; Jaiswal, J. K.; Hurley, D. G.; Liyanage, H. D. S.; Mcmanaway, S. P.; Gu, Y.; Richter, S.; Wang, J.; Tercel, M.; Print, C. G.; Wilson, W. R.; Pruijn, F. B., The Flavoprotein FOXRED2 Reductively Activates Nitro-chloromethylbenzindolines and other Hypoxia-Targeting Prodrugs. *Biochem. Pharmacol.* **2014,** *89*, 224–235.

[40] Guise, C. P.; Abbattista, M. R.; Singleton, R. S.; Holford, S. D.; Connolly, J.; Dachs, G. U.; Fox, S. B.; Pollock, R.; Harvey, J.; Guilford, P.; Doñate, F.; Wilson, W. R.; Patterson, A. V., The Bioreductive Prodrug PR-104A Is Activated under Aerobic Conditions by Human Aldo-Keto Reductase 1C3. *Cancer Res.* **2010,** *70* (4), 1573–1584.

[41] Hunter, F. W.; Wouters, B. G.; Wilson, W. R., Hypoxia-activated prodrugs: paths forward in the era of personalised medicine. *Br. J. Cancer* **2016,** *114* (10), 1071-1077.

[42] Jung, D.; Jiao, H.; Duan, J.-X.; Matteucci, M.; Wang, R., Metabolism, Pharmacokinetics and Excretion of a Novel Hypoxia Activated Cytotoxic Prodrug, TH-302, in Rats. *Xenobiotica* **2012,** *42* (4), 372–388.

[43] Duan, J.-X.; Jiao, H.; Kaizerman, J.; Stanton, T.; Evans, J. W.; Lan, L.; Lorente, G.; Banica, M.; Jung, D.; Wang, J.; Ma, H.; Li, X.; Yang, Z.; Hoffman, R. M.; Ammons, W. S.; Hart, C. P.; Matteucci, M., Potent and Highly Selective Hypoxia-Activated Achiral Phosphoramidate Mustards as Anticancer Drugs. *J. Med. Chem.* **2008,** *51*, 2412–2420.

[44] Sun, J. D.; Liu, Q.; Wang, J.; Ahluwalia, D.; Ferraro, D.; Wang, Y.; Duan, J.-X.; Ammons, W. S.; Curd, J. G.; Matteucci, M. D.; Hart, C. P., Selective Tumor Hypoxia Targeting by Hypoxia-Activated Prodrug TH-302 Inhibits Tumor Growth in Preclinical Models of Cancer. *Clin. Cancer. Res.* **2012,** *18* (3), 758–770.

[45] Su, J.; Gu, Y.; Pruijn, F. B.; Smaill, J. B.; Patterson, A. V.; Guise, C. P.; Wilson, W. R., Zinc Finger Nuclease Knock-out of NADPH:Cytochrome P450 Oxidoreductase (POR) in Human Tumor Cell

Lines Demonstrates That Hypoxia-activated Prodrugs Differ in POR Dependence. *J. Biol. Chem.* **2013,** *288* (52), 37138–37153.

[46] Hay, M. P.; Anderson, R. F.; Ferry, D. M.; Wilson, W. R.; Denny, W. A., Synthesis and Evaluation of Nitroheterocyclic Carbamate Prodrugs for Use with Nitroreductase-Mediated Gene-Directed Enzyme Prodrug Therapy. *J. Med. Chem.* **2003,** *46*, 5533–5545.

[47] Kim, E. Y.; Liu, Y.; Akintujoye, O. M.; Shyam, K.; Grove, T. A.; Sartorelli, A. C.; Rockwell, S., Preliminary Studies with a New Hypoxia-Selective Cytotoxin, KS119W, In Vitro and In Vivo. *Radiat. Res.* **2012,** *178* (3), 126–137.

[48] Penketh, P. G.; Baumann, R. P.; Shyam, K.; Williamson, H. S.; Ishiguro, K.; Zhu, R.; Eriksson, E. S. E.; Eriksson, L. A.; Sartorelli, A. C., 1,2-Bis(methylsulfonyl)-1-(2-chloroethyl)-2-[[1-(4-nitrophenyl)ethoxy]carbonyl]hydrazine (KS119): A Cytotoxic Prodrug with Two Stable Conformations Differing in Biological and Physical Properties. *Chem. Biol. Drug Des.* **2011,** *78*, 513–526.

[49] Seow, H. A.; Penketh, P. G.; Shyam, K.; Rockwell, S.; Sartorelli, A. C., 1,2-Bis(methylsulfonyl)-1-(2-chloroethyl)-2-[[1-(4-nitrophenyl)ethoxy]carbonyl]hydrazine: An Anticancer Agent Targeting Hypoxic Cells. *Proc. Natl. Acad. Sci. U. S. A.* **2005,** *102* (26), 9282–9287.

[50] Penketh, P. G.; Shyam, K.; Zhu, R.; Baumann, R. P.; Ishiguro, K.; Sartorelli, A. C., Influence of Phosphate and Phosphoesters on the Decomposition Pathway of 1,2-Bis(methylsulfonyl)-1-(2-chloroethyhydrazine (90CE), the Active Anticancer Moiety Generated by Laromustine, KS119, and KS119W. *Chem. Res. Toxicol.* **2014,** *27* (5), 818–833.

[51] Baumann, R. P.; Penketh, P. G.; Ishiguro, K.; Shyam, K.; Zhu, Y. L.; Sartorelli, A. C., Reductive Activation of the Prodrug 1,2-Bis(methylsulfonyl)-1-(2-chloroethyl)-2-[[1-(4-nitrophenyl)ethoxy]carbonyl]hydrazine (KS119) Selectively Occurs in Oxygen-Deficient Cells and Overcomes O^6-Alkylguanine-DNA Alkyltransferase Mediated KS119 Tumor Cell Resistance. *Biochem. Pharmacol.* **2010,** *79* (11), 1553–1561.

[52] Shyam, K.; Penketh, P. G.; Shapiro, M.; Belcourt, M. F.; Loomis, R. H.; Rockwell, S.; Sartorelli, A. C., Hypoxia-Selective Nitrobenzyloxycarbonyl Derivatives of 1,2-Bis(methylsulfonyl)-1-(2-chloroethyl)hydrazines. *J. Med. Chem.* **1999,** *42* (5), 941–946.

[53] Paine, M. J. I.; Garner, A. P.; Powell, D.; Sibbald, J.; Sales, M.; Pratt, N.; Smith, T.; Tew, D. G.; Wolf, C. R., Cloning and Characterization of a Novel Human Dual Flavin Reductase. *J. Biol. Chem.* **2000,** *275*, 147150–591478.

[54] Garner, A. P.; Paine, M. J. I.; Rodriguez-Crespo, I.; Chinje, E. C.; Montellano, P. O. D.; Stratford, I. J.; Tew, D. G.; Wolf, C. R., Nitric Oxide Synthases Catalyze the Activation of Redox Cycling and Bioreductive Anticancer Agents. *Cancer Res.* **1999,** *59*, 1929–1934.

[55] Aigrain, L.; Fatemi, F.; Frances, O.; Lescop, E.; Truan, G., Dynamic Control of Electron Transfers in Diflavin Reductases. *Int. J. Mol. Sci.* **2012,** *13*, 15012–15041.

[56] Finn, R. D.; Basran, J.; Roitel, O.; Wolf, C. R.; Munro, A. W.; Paine, M. J. I.; Scrutton, N. S., Determination of the Redox Potentials and Electron Transfer Poperties of the FAD- and FMN-Bnding Dmains of the Hman Oidoreductase NR1. *Eur. J. Biochem.* **2003,** *270*, 1164–1175.

[57] Munro, A. W.; Noble, M. A.; Robledo, L.; Daff, S. N.; Chapman, S. K., Determination of the Redox Properties of Human NADPH-Cytochrome P450 Reductase. *Biochemistry* **2001,** *40*, 1956–1963.

[58] Gao, Y. T.; Smith, S. M. E.; Weinberg, J. B.; Montgomery, H. J.; Newman, E.; Guillemette, J. G.; Ghosh, D. K.; Roman, L. J.; Martasek, P.; Salerno, J. C., Thermodynamics of Oxidation-Reduction Reactions in Mammalian Nitric-oxide Synthase Isoforms. *J. Biol. Chem.* **2004,** *279*, 18759–18766.

[59] Wolthers, K. R.; Basran, J.; Munro, A. W.; Scrutton, N. S., Molecular Dissection of Human Methionine Synthase Reductase: Determination of the Flavin Redox Potentials in Full-Length Enzyme and Isolated Flavin-Binding Domains. *Biochemistry* **2003,** *42* (13), 3911–3920.

[60] Stuehr, D. J.; Santolini, J.; Wang, Z.-Q.; Wei, C.-C.; Adak, S., Update on Mechanism and Catalytic Regulation in the NO Synthases. *J. Biol. Chem.* **2004,** *279*, 36167–36170.
[61] Olteanu, H.; Banerjee, R., Human Methionine Synthase Reductase, a Soluble P-450 Reductase-like Dual Flavoprotein, Is Sufficient for NADPH-dependent Methionine Synthase Activation. *J. Biol. Chem.* **2001,** *276* (38), 35558–35563.
[62] Riddick, D. S.; Ding, X.; Wolf, C. R.; Porter, T. D.; Pandey, A. V.; Zhang, Q.-Y.; Gu, J.; Finn, R. D.; Ronseaux, S.; Mclaughlin, L. A.; Henderson, C. J.; Zou, L.; Flück, C. E., NADPH–Cytochrome P450 Oxidoreductase: Roles in Physiology, Pharmacology, and Toxicology. *Drug Metab. Disposition* **2013,** *41*, 12–23.
[63] Patterson, A.; Barham, H.; Chinje, E.; Adams, G.; Harris, A.; Stratford, I., Importance of P450 Reductase Activity in Determining Sensitivity of Breast Tumour Cells to the Bioreductive Drug, Tirapazamine (SR 4233). *Br. J. Cancer* **1995,** *72*, 1144–1150.
[64] Finn, R. D.; Wilkie, M.; Smith, G.; Paine, M. J. I., Identification of a functionally impaired allele of human novel oxidoreductase 1 (NDOR1), NDOR1*1. *Pharmacogenet. Genomics* **2005,** *15* (6), 381-386.
[65] Olteanu, H.; Banerjee, R., Redundancy in the Pathway for Redox Regulation of Mammalian Methionine Synthase REDUCTIVE ACTIVATION BY THE DUAL FLAVOPROTEIN, NOVEL REDUCTASE 1. *J. Biol. Chem.* **2003,** *278*, 38310–38314.
[66] Guan, Z.-W.; Kamatani, D.; Kimura, S.; Iyanagi, T., Mechanistic Studies on the Intramolecular One-electron Transfer between the Two Flavins in the Human Neuronal Nitric-oxide Synthase and Inducible Nitric-oxide Synthase Flavin Domains. *J. Biol. Chem.* **2003,** *278*, 30859–30868.
[67] Thomsen, L. L.; Miles, D. W.; Happerfield, L.; Bobrow, L. G.; Knowles, R. G.; Moncada, S., Nitric Oxide Synthase Activity in Human Breast Cancer. *Br. J. Cancer* **1995,** *72*, 41–44.
[68] Swana, H. S.; Smith, S. D.; Perrotta, P. L.; Saito, N.; Wheeler, M. A.; Weiss, R. M., Inducible Nitric Oxide Synthase with Transitional Cell Carcinoma of the Bladder. *J. Urol.* **1999,** *161* (2), 630–634.
[69] Chandor, L.; Dijols, S.; Ramassamy, B.; Frapart, Y.; Mansuy, D.; Stuehr, D.; Helsby, N.; Boucher, J.-L., Metabolic Activation of the Antitumor Drug 5-(Aziridin-1-yl)-2,4-Dinitrobenzamide (CB1954) by NO Synthases. *Chem. Res. Toxicol.* **2008,** *21* (4), 836–843.
[70] Chinje, E. C.; Cowen, R. L.; Feng, J.; Sharma, S. P.; Wind, N. S.; Harris, A. L.; Stratford, I. J., Non-Nuclear Localized Human NOSII Enhances the Bioactivation and Toxicity of Tirapazamine (SR4233) in Vitro. *Mol. Pharmacol.* **2003,** *63* (6), 1248–1255.
[71] Riemer, J.; Appenzeller-Herzog, C.; Johansson, L.; Bodenmiller, B.; Hartmann-Petersen, R.; Ellgaard, L., A Luminal Flavoprotein in Endoplasmic Reticulum-Associated Degradation. *Proc. Natl. Acad. Sci. U. S. A.* **2009,** *106* (35), 14831–14836.
[72] Riemer, J.; Hansen, H. G.; Appenzeller-Herzog, C.; Johansson, L.; Ellgaard, L., Identification of the PDI-Family Member ERp90 as an Interaction Partner of ERFAD. *PLoS One* **2011,** *6* (2), e17037.
[73] Penning, T. M.; Drury, J. E., Human Aldo–Keto Reductases: Function, Gene Regulation, and Single Nucleotide Polymorphisms. *Arch. Biochem. Biophys.* **2007,** *464* (2), 241–250.
[74] Pizzolato, J. F.; Saltz, L. B., The Camptothecins. *The Lancet* **2003,** *361* (9376), 2235–2242.
[75] Staker, B. L.; Hjerrild, K.; Feese, M. D.; Behnke, C. A.; Burgin Jr, A. B.; Stewart, L., The Mechanism of Topoisomerase I Poisoning by a Camptothecin Analog. *Proc. Natl. Acad. Sci. U. S. A.* **2002,** *99* (24), 15387–15392.
[76] Rapisarda, A.; Uranchimeg, B.; Scudiero, D. A.; Selby, M.; Sausville, E. A.; Shoemaker, R. H.; Melillo, G., Identification of Small Molecule Inhibitors of Hypoxia-inducible Factor 1 Transcriptional Activation Pathway. *Cancer Res.* **2002,** *62*, 4316–4324.

[77] Bertozzi, D.; Marinello, J.; Manzo, S. G.; Fornari, F.; Gramantieri, L.; Capranico, G., The Natural Inhibitor of DNA Topoisomerase I, Camptothecin, Modulates HIF-1α Activity by Changing miR Expression Patterns in Human Cancer Cells. *Mol. Cancer Ther.* **2014,** *13*, 239–248.

[78] Marchand, C.; Antony, S.; Kohn, K. W.; Cushman, M.; Ioanoviciu, A.; Staker, B. L.; Burgin, A. B.; Stewart, L.; Pommier, Y., A Novel Norindenoisoquinoline Structure Reveals a Common Interfacial Inhibitor Paradigm for Ternary Trapping of the Topoisomerase I-DNA Covalent Complex. *Mol. Cancer Ther.* **2006,** *5* (2), 287–295.

[79] Strumberg, D.; Pilon, A. A.; Smith, M.; Hickey, R.; Malkas, L.; Pommier, Y., Conversion of Topoisomerase I Cleavage Complexes on the Leading Strand of Ribosomal DNA into 5'-Phosphorylated DNA Double-Strand Breaks by Replication Runoff. *Mol. Cell. Biol.* **2000,** *20* (11), 3977–3987.

[80] Guérin, E.; Raffelsberger, W.; Pencreach, E.; Maier, A.; Neuville, A.; Schneider, A.; Bachellier, P.; Rohr, S.; Petitprez, A.; Poch, O.; Moras, D.; Oudet, P.; Larsen, A. K.; Gaub, M.-P.; Guenot, D., In Vivo Topoisomerase I Inhibition Attenuates the Expression of Hypoxia-Inducible Factor 1α Target Genes and Decreases Tumor Angiogenesis. *Mol. Med.* **2012,** *18*, 83–94.

[81] Fabian, M. R.; Sonenberg, N.; Filipowicz, W., Regulation of mRNA Translation and Stability by microRNAs. *Annu. Rev. Biochem* **2010,** *79* (1), 351–379.

[82] Liang, H.; Wu, X.; Yalowich, J. C.; Hasinoff, B. B., A Three-Dimensional Quantitative Structure-Activity Analysis of a New Class of Bisphenol Topoisomerase IIα Inhibitors. *Mol. Pharmacol.* **2008,** *73* (3), 686-696.

[83] Hasinoff, B. B.; Creighton, A. M.; Kozlowska, H.; Thampatty, P.; Allan, W. P.; Yalowich, J. C., Mitindomide Is a Catalytic Inhibitor of DNA Topoisomerase II That Acts at the Bisdioxopiperazine Binding Site. *Mol. Pharmacol.* **1997,** *52* (5), 839-845.

[84] Connelly, N. G.; Geiger, W. E., Chemical Redox Agents for Organometallic Chemistry. *Chem. Rev.* **1996,** *96* (2), 877-910.

[85] Pavlishchuk, V. V.; Addison, A. W., Conversion constants for redox potentials measured versus different reference electrodes in acetonitrile solutions at 25°C. *Inorg. Chim. Acta* **2000,** *298* (1), 97-102.

[86] Kuhn, A.; Von Eschwege, K. G.; Conradie, J., Reduction potentials of para-substituted nitrobenzenes—an infrared, nuclear magnetic resonance, and density functional theory study. *J. Phys. Org. Chem.* **2012,** *25* (1), 58-68.

[87] O'connor, L. J.; Cazares-Korner, C.; Saha, J.; Evans, C. N. G.; Stratford, M. R. L.; Hammond, E. M.; Conway, S. J., Efficient synthesis of 2-nitroimidazole derivatives and the bioreductive clinical candidate Evofosfamide (TH-302). *Organic Chemistry Frontiers* **2015,** *2* (9), 1026-1029.

[88] O'connor, L. J.; Cazares-Korner, C.; Saha, J.; Evans, C. N. G.; Stratford, M. R. L.; Hammond, E. M.; Conway, S. J., Design, synthesis and evaluation of molecularly targeted hypoxia-activated prodrugs. *Nat. Protocols* **2016,** *11* (4), 781-794.